

Constraints on the origin of gabbroic rocks from the Moldanubian-Moravian units boundary (Bohemian Massif, Czech Republic and Austria)

JAROMÍR ULRYCH^{1*}, LUKÁŠ ACKERMAN¹, VÁCLAV KACHLÍK², ERNST HEGNER³, KADOSA BALOGH⁴, ANNA LANGROVÁ¹, JAN LUNA⁵, FERRY FEDIUK⁶, MILOŠ LANG¹ and JIŘÍ FILIP¹

¹Institute of Geology v.v.i., Academy of Sciences of the Czech Republic, Rozvojová 269, 165 00 Praha 6, Czech Republic; ulrych@gli.cas.cz

²Faculty of Science, Charles University, Albertov 6, 128 43 Praha 2, Czech Republic

³Department of Geowissenschaften, Universität München, Theresienstraße 41, D-80333 München, Germany

⁴Institute of Nuclear Research, Hungarian Academy of Sciences, Bemtér 18/C, H-4026 Debrecen, Hungary

⁵Jihlava, Březinova 41, 58 601 Jihlava, Czech Republic

⁶Geohelp, Na Petřínách 1897, 162 00 Praha 6, Czech Republic

(Manuscript received May 29, 2009; accepted in revised form December 11, 2009)

Abstract: Gabbroic bodies from the Moldanubian Monotonous Group (Maříž) and the Moravian Vratěnín Unit (other sites), often showing retrogressive recrystallization at their margins in the amphibolite-facies grade, have norite, gabbro, and hornblende compositions. Gabbros with preserved coronitic textures are limited to the Vratěnín Unit. The estimated equilibration temperatures derived from plagioclase–amphibole pairs and orthopyroxene Ca contents calculated for pressures 5–10 kbar overlap for coronitic (700–840 °C) and non-coronitic gabbroic rocks (680–850 °C). Although the Moldanubian (Maříž) gabbroic rocks are more Mg-rich compared to the Moravian gabbroids, they show crust-like La/Nb ratios of 2.1–6.6 characteristic of subduction-related magmatic rocks coupled with uniform low ϵ_{Nd} values of +0.6 to +0.7. Apparent subduction-related features are probably caused by contamination by juvenile crust and/or by metamorphic fluid rich in incompatible elements during the Variscan metamorphism. Samples from Korolupy–Nonndorf and Mešovice have La/Nb ratios < 1.7 and show negative correlations between La/Nb and ϵ_{Nd} . Such decoupling between La/Nb and ϵ_{Nd} could be attributed to contamination of the subduction-related parent magma by crustal material with higher La/Nb and lower ϵ_{Nd} values. Samples from Uherčice show ambiguous geochemical patterns inherited from contamination by very old recycled material. Gabbroic rocks from Maříž should represent an underplated, partly layered cumulate body of continental tholeiite composition, strongly influenced by crustal contamination. In contrast, gabbroic bodies from the Vratěnín Unit, having a close spatial relationship to the surrounding garnet amphibolites, were emplaced into a lithologically variable passive margin sequence probably during the Cadomian extension.

Key words: Bohemian Massif, Moldanubian Unit, Moravian Unit, Sr-Nd isotopes, K-Ar ages, geochemistry, gabbroic rocks.

Introduction

Gabbros and norites represent either products of middle stages of fractionation of a basaltic magma in layered complexes or differentiated sills. Gabbroic rocks in orogenic batholiths, composed of members of the gabbro–diorite–tonalite–monzonite–granodiorite–granite calc-alkaline suite, can compose 7–14 vol. % of the whole (Pitcher 1978). They also occur in intrusions (partly of alkali character) in extensional settings with members of a granite–syenite trend or as members of the gabbro–anorthosite–charnockite suite (2–10 vol. % only — Vorma 1976). Phanerozoic gabbroic rocks also form minor components of alkalic anorogenic suites related to crustal doming and rifting (e.g. the Oslo Rift — Neumann 1978).

We present results on (ultra)mafic gabbroic bodies from: 1. the Monotonous Group of the Moldanubian Unit in close spatial relationship with the Moldanubian pluton and 2. the tectonic slice of the Vratěnín Varied Unit of the Moravian affinity, stacked in the Drosendorf window together with HP-HT rocks of the Gföhl Unit and with MP-MT rocks of the

Podhradí Unit (Jenček & Dudek 1971; Racek et al. 2006) adjacent to the major thrust boundary with the underlying Brunovistulian block. The Moldanubian pluton intruded the paragneisses and migmatites of the Monotonous Unit in the time span of ca. 330–280 Ma (Finger et al. 1997; Gerdes et al. 2000). The main gabbroic and dioritic bodies occurring in this region (Group II of Koller 1998) occur as stockwork-like intrusions or lens-like bodies, less than 1 km in size, within both granites and gneisses. Additionally, small inclusions of similar composition occur within the granite (Group I of Koller l.c.) from 5 cm to 2 m in diameter.

Geological settings

The Bohemian Massif represents a part of the Variscan orogenic belt formed during the collision of Gondwana, Laurasia and associated microcontinents (e.g. Franke 2000; Matte 2001). It consists of four different crustal segments of the Peri-Gondwanan affinity: (1) Moldanubian, (2) Saxothuringian, (3) Teplá-Barrandian, and (4) Moravo-Silesian.

The studied gabbroic bodies occur in a complicated tectonic stack of the Moldanubian and Moravian units (called the Drosendorf stack — Tollman 1982) in close proximity to the major thrust boundary between the Moldanubian high-grade gneisses and Cadomian Brunovistulian foreland (cf. different genetic interpretations — see discussion in Schulmann et al. 2005). The E-W profile through the classical Drosendorf window with gabbros and retrogressed metagabbros illustrates the pre-Variscan geodynamic setting of individual crustal slices. From the top to the bottom, the following lithotectonic units (only those containing the studied gabbroic rocks) can be distinguished (see Fig. 1):

a) The Monotonous Unit formed by migmatitic paragneisses with cordierite close to the contact with the Variscan gran-

itoids. U-Pb dating of clastic zircons from paragneisses shows a maximum Neoproterozoic sedimentary age for these units (Kröner et al. 1988). The layered gabbro from Maříž crops out in the western part of this unit near the contact with the Moldanubian pluton. The gabbroic bodies range from 60 to 600 m in size and occur (in particular those near Maříž) along the southern continuation of the Přibyslav Mylonite Zone.

b) The Vratěnin Varied Unit is composed of paragneisses with frequent intercalation of marbles, graphite paragneisses and garnet amphibolites with pyroxene relicts. Gabbroic rocks form bodies X0 m in size in the surrounding paragneisses W and SW of Korolupy and Nonndorf and between Uherčice and Mešovice, where gabbros are spatially associated with amphibolites, calc-silicate rocks and marbles. Relatively fresh

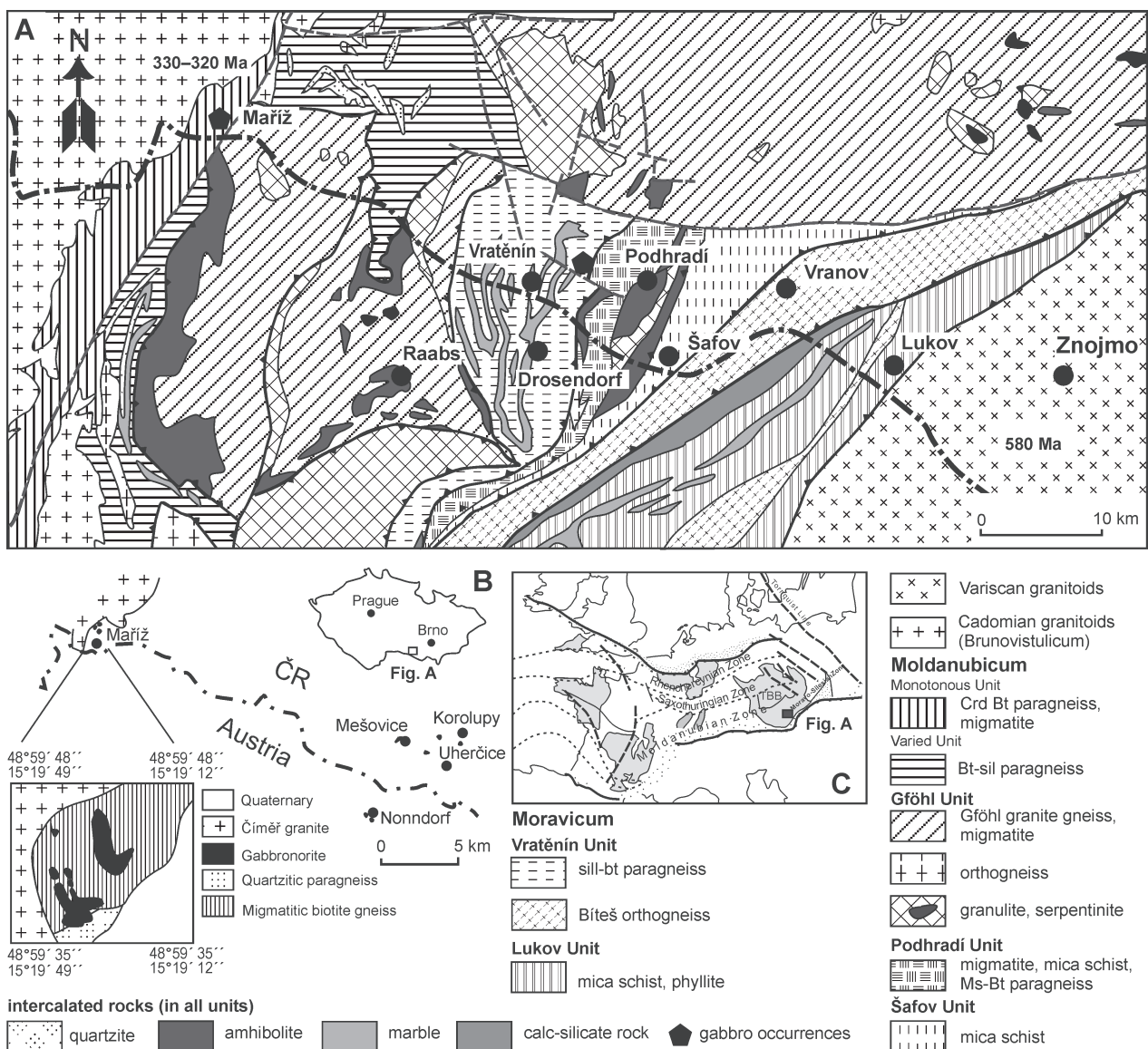


Fig. 1. A — Geological map of the Moldanubian/Moravian units boundary (modified after map 1:500,000 — Cháb et al. 2007); **B** — Sketch map of the occurrences of the studied gabbroic rocks from the Moravia/Austria border, (B) the map of the Maříž gabbroic body 1:4,000 based on new geological studies and geomagnetic measurements; **C** — Location of studied area in the frame of major zones of the Variscan orogen (marked by a dark rectangle).

olivine and pyroxene gabbros and ultramafic cumulates associated with gabbros in Korolupy and Mešovice bodies pass to amphibolitized gabbros and fine-grained gabbroamphibolites with only scarce relics of pyroxenes. This unit was considered an equivalent of the Vranov-Olešnice Unit of the Moravicum (Jenček & Dudek 1971) or correlated with the Moldanubian Varied Unit (Schulmann et al. 2005; Racek et al. 2006). Jenček & Dudek (1971) supposed an early Variscan age for the gabbros, but without any radiometric evidence.

Methods

Special attention was applied to the positions and shape of the inhomogeneous Maříž gabbroic body occurring at the immediate contact with the Moldanubian pluton. Magnetometric measurements (57,000 m² with 7,500 of point measurements) were performed using the method of magnetometric gradiometry and the Envi Scintrex proton magnetometer.

Whole-rock major element concentrations were determined at the Charles University, Prague, using wet chemical methods. Analyses of the reference standards (GM, TB, BN) and duplicate analyses of the samples yield total errors of $\pm 5\%$ (1 σ). A quadrupole-based ICP-MS (VG Elemental PQ3) was used for determination of REE and other trace elements using the methods of Strnad et al. (2005). The accuracy was tested against reference rock standard BCR-2, the precision was monitored by replicate analyses of the same reference material and was always better than $\pm 5\%$ (1 σ).

Mineral analyses were carried out on a Cameca SX 100 electron microprobe using the wavelength-dispersive spectrometry (WDS) analyser at the Institute of Geology, Academy of Sciences of the Czech Republic. Analytical conditions were as follows: 15 kV accelerating voltage, 10 nA beam current and 2 μ m beam diameter. A counting time of 10 s was used for all elements. Synthetic and natural minerals were used as standards. Data reduction used the X-PHI Merlet correction (Merlet 1992).

The K-Ar isotope measurements were carried out at the Institute of Nuclear Research of the Hungarian Academy of Sciences, Debrecen, according to the

Table 1: List of samples of the gabbroic rocks with location and petrographic characteristics.

Sample No.	Latitude °N	Longitude °E	Locality and its geological characteristic	Rock type	Petrographic characteristic	Mineralogy
M-1b	48.880	15.564	Nonndorf: two elliptical bodies (350 by 150 m and 150 by 90 m) in biotite gneisses of the Moldanubian Unit. The abandoned pit quarry is situated in a larger body in the close neighbourhood of the village	Olivine norite hornblende-bearing	Gabbroplitic coronitic texture around olivine	Plg>Opx-Ol>>Hbl (brown)>>(Phl)
M-2	48.928	15.626	Korolupy (Kurlupp): elliptical body (220 by 150 m) is embedded in biotite gneisses of the Moldanubian Unit. Abandoned pit quarry is situated 1.8 km E of the village	Norite hornblende-bearing	Gabbroplitic coronitic texture mostly around orthopyroxene, partly also olivine	Plg-Opx>>Hbl (brown)>>(Ol, Phl)
M-3A	48.923	15.641	Uherčice: tectonized small isometric body (80 by 80 m) in biotite gneisses with marble intercalations of the Moldanubian Unit. Boulders in the field situated 1.2 km N of the village	Hornblende melagabbro	Subhedral-granular texture	Opx>Hbl (brown)-Plg>>Cpx, (Ga)
M-3B	48.923	15.641	Uherčice: the same locality	Hornblende melagabbro	Gabbroic fine-grained mosaic texture	Hbl (pale green) >>Plg >>Cpx
M-4	48.994	15.614	Mešovice: N-S – elongated elliptical body (600 by 200 m) in biotite gneisses and garnet amphibolite of the Moldanubian Unit. Boulders on the field situated 1.5 km E of the village	Hornblende norite to gabbroamphibolite	Gabbroic unequally-grained texture, partly oriented structure	Hbl (brown-green) ~ Plg >>Cpx
M-5-1	48.996	15.316	Maříž: two irregular N-S elongated elliptical bodies (150 by 100 m and 150 by 75 m) at the contact of the Moldanubian pluton and the Moldanubian Unit formed by migmatites and quartz gneisses. The main textural type at the locality. Boulders on a field situated 0.8 km N of the village. For geological location see Fig. 1.	Hornblende olivine gabbronorite	Gabbroic to gabbroplitic texture	Plg-Hbl (brown) > Opx-Cpx >>Ol >K-f
M-5-2	48.995	15.316	Maříž: the same locality; minor rock type of the bodies	Gabbronorite	Gabbroic texture	Plg>Opx>>Cpx
M-5-3	48.996	15.316	Maříž: the same locality; minor rock type of the bodies	Biotite gabbro hornblende-bearing	Subhedral-granular texture	Plg~Bt>Hbl~Cpx
M-5-4	48.995	15.316	Maříž: the same locality; minor rock type of the bodies	Olivine hornblende (uralitized)	Anhedral-granular texture. Ultramafic rock free of feldspars	Hbl (uralite) >O>>>Ore minerals
M-5-5	48.994	15.316	Maříž: the same locality; minor rock type of the bodies	Hornblende gabbro biotite-bearing	Gabbroic texture	Hbl (brown)>>green ~Plg>>Bt
M-6	49.060	15.090	Čiměř: granite of the Čiměř type is one of the prevailing granitic rock types of the Moldanubian pluton, in spatial association with the gabbroic body of Maříž. The quarry is situated 1 km E of the village	Two-mica granite (monzogranite)	Slightly porphyritic texture; subhedral-granular texture	K-f (microcline) ~Plg ~Q>>Mu~Bt

procedures described in Balogh (1985), results of an interlaboratory calibration have been presented by Odin (Ed.) (1982). Standards LP-6 and HD-B1 have been used to calibrate the measurement of $^{40}\text{Ar}/\text{rad}$ and K concentrations and atmospheric argon for checking the determination of Ar isotopic ratios. Atomic constants according to Steiger & Jäger (1977) have been used for calculation of ages.

Apatite fission-track analysis (AFTA) was undertaken to determine the age and the thermal history of gabbroic and spatially-associated granite. The external detector method was used for fission-track analysis.

The Sm-Nd isotopic work was carried out in the isotope laboratory at the Universität München according to the procedures outlined in Hegner et al. (1995). The isotopic measurements were carried out on a MAT 261 in a dynamic quadrupole mass collection mode. The $^{143}\text{Nd}/^{144}\text{Nd}$ ratios were normalized to $^{146}\text{Nd}/^{144}\text{Nd}=0.7219$. The external precision of the $^{143}\text{Nd}/^{144}\text{Nd}$ ratios is 1.2×10^{-5} as has been confirmed with an Ames Nd standard solution yielding 0.512142 ± 12 ($N=35$), corresponding to 0.511854 in the La Jolla Nd reference standard material. The ϵ_{Nd} values were calculated with the parameters of Jacobsen & Wasserburg (1980). Present-day values for the chondrite uniform reservoir (CHUR): $^{147}\text{Sm}/^{144}\text{Nd}=0.1967$, $^{143}\text{Nd}/^{144}\text{Nd}=0.512638$ (Jacobsen & Wasserburg 1980; $^{143}\text{Nd}/^{144}\text{Nd}$ re-normalized to $^{146}\text{Nd}/^{144}\text{Nd}=0.7219$). $^{87}\text{Sr}/^{86}\text{Sr}$ ratios were measured in a dynamic double cup mass collection mode and normalized to $^{86}\text{Sr}/^{88}\text{Sr}=0.1194$. The NIST 987 reference material yielded $^{87}\text{Sr}/^{86}\text{Sr}=0.71022$ ($N=22$).

Sampled localities and petrography

The list of the rocks and their location is presented in Table 1, together with their concise petrographical characteristics. The rock names correspond to the modal classification of Le Maitre (Ed.) (2002). Geographical coordinates of individual rock samples are presented in Table 1 and quantitative modal compositions in Table 2. Prevailing primary magmatic rock-forming mineral assemblages of most of the gabbroic rocks

are variably overprinted during the later metamorphic processes. Depending on fluid activity, coronitic gabbros from the Vratěnín Unit with preserved original magmatic ophitic to gabbroophitic textures were variably recrystallized to gabbroamphibolites where pyroxene is mostly replaced by different amphibole species. Plagioclase is also recrystallized and variably equilibrated into a mosaic of newly formed grains. Some samples from Maříž and Mešovice are recrystallized to relatively fine-grained gabbroamphibolites, where only several relicts of unaltered pyroxene have been preserved. These microstructures show that recrystallization occurred in the amphibolite facies grade.

Compositional layering on a centimeter scale of some samples from Maříž show that cumulation of olivine- and/or orthopyroxene-rich and feldspar-rich layers played an important role in the differentiation of the parent magma.

Rock-forming minerals

Olivine is ubiquitous, in particular in the olivine norite from Nonndorf, more rarely also Korolupy. It forms subhedral grains (Fo_{60-50}) concentrated in the centers of coronitic textures (Fig. 2A). Subhedral olivines in the matrix are less magnesian ($\sim\text{Fo}_{50}$). More magnesian olivine (Fo_{65-80} , cf. data in Table 3) also occurs in substantial amounts in the olivine gabbronorite (M-5-1) and olivine hornblendite (M-5-4) from Maříž.

Orthopyroxene (En_{70-60}) is common in the Korolupy and Nonndorf norites, concentrated in the centers (Fig. 2B) or forming the rims of olivine in coronitic textures (Fig. 2A). Its rarer presence in the Nonndorf samples (En_{70-60} , rare rims up to En_{45}) is compensated for by the substantial amount of olivine in the same structural position in the coronitic textures. Maximum concentrations of orthopyroxene occur in the Maříž gabbronorite (M-5-2) where compositions vary from enstatite (En_{80-70}) to rare rims of ferrosilite (En_{45}) (cf. Fig. 3 and Table 4). Uralitization of orthopyroxenes is common. **Clinopyroxene** occurs ubiquitously in the gabbroic rocks. It forms over 40 vol. % in the Uherčice melanorites (M-3A) and sub-

Table 2: Modal composition of the gabbroic rocks (in vol. %).

Sample No.	M-1b	M-2	M-3A	M-3B	M-4	M-5-1	M-5-2	M-5-3	M-5-4	M-5-5	M-6
Olivine	20	2	0	0	0	8	0	0	30	0	0
Orthopyroxene	25	38	0	0	3	14	34	0	4	0	0
Clinopyroxene	0	0	43	8	0	12	11	8	0	0	0
Amphibole brown	5	7	35	0	51	28	2	13	0	47	0
Amphibole (light) green	0	0	0	62	0	0	0	0	61	5	0
Garnet	0	1	2	0	0	0	0	0	0	0	0
Dark mica	2	2	0	0	0	2	1	35	0	5	7
Muscovite	0	0	0	0	0	0	0	0	0	0	8
Plagioclase	45	47	20	29	38	31	49	40	0	41	25
K-feldspar	0	0	0	0	0	4	0	0	0	0	28
Quartz	0	0	0	0	0	0	0	0	0	0	32
Ore minerals	2	3	tr.	1	5	1	3	1	5	2	tr.
Titanite	0	0	0	0	2	0	0	1	0	0	0
Apatite	1	0	0	0	1	0	0	2	0	0	tr.
Total	100	100	100	100	100	100	100	100	100	100	100
Number of analytical points	950	1000	900	950	1000	1200	1000	1000	1100	1100	980

In samples Nos. M-5-1 and M-5-3 (both from Maříž), the presence of small amounts of cummingtonite has been microscopically stated; tr. — traces

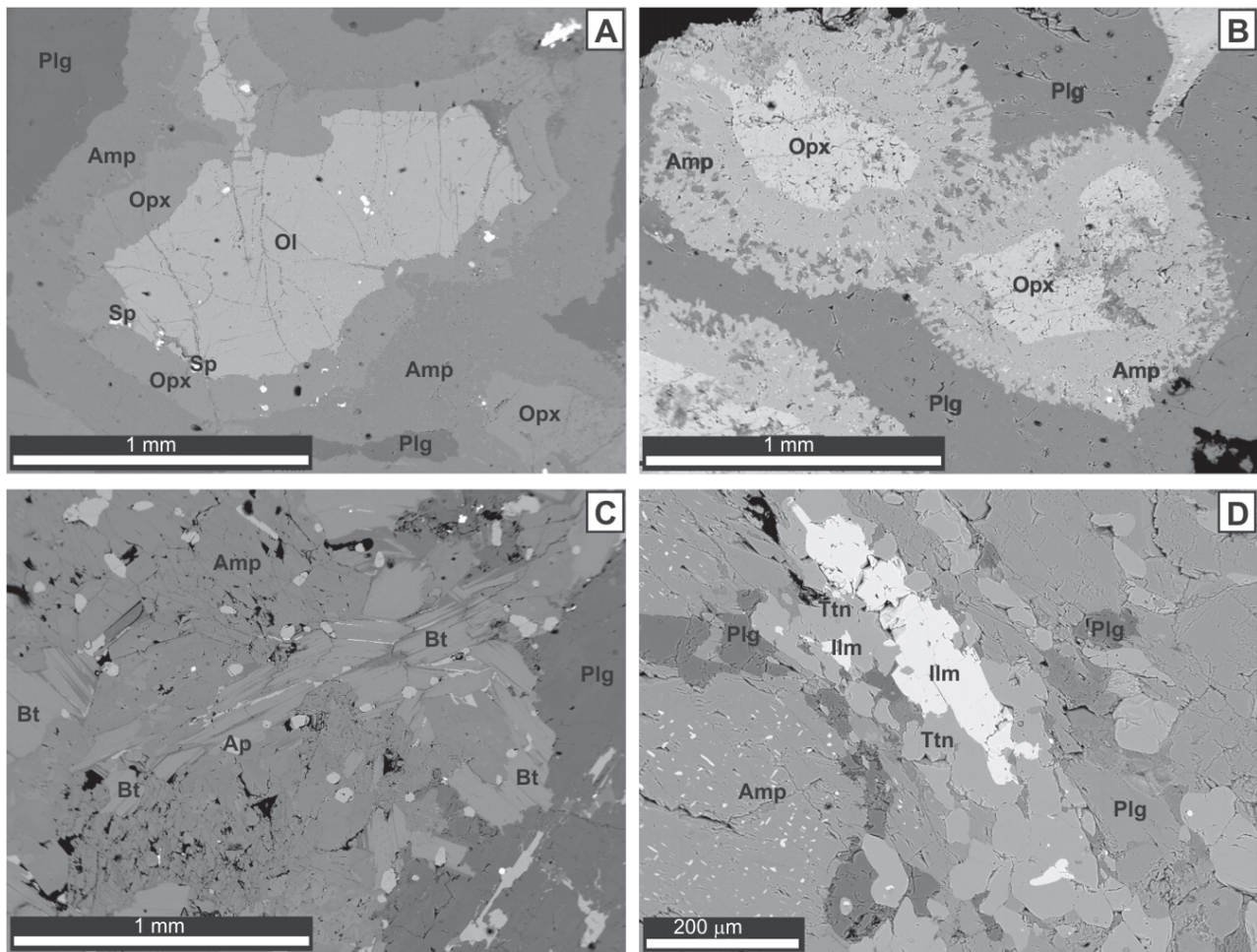


Fig. 2. Back-scattered electron image (Cameca SX-100): **A** — Coronitic texture of olivine norite from Nonndorf. Olivine (Ol) in the centre of the coronitic texture is rimmed by orthopyroxene (Opx) of enstatite and amphibole (Amp) of pargasite compositions. Chromium spinel (Sp) occurs along the olivine-orthopyroxene boundary. Plagioclase (Plg) is of labradorite composition. **B** — Coronitic texture of norite from Korolupy. Orthopyroxene (Opx) of enstatite composition in centres of coronite texture is rimmed by pargasite (Amp) with a marginal zone of intergrowths with plagioclase (Plg) of labradorite composition. **C** — Younger biotite (Bt) laths penetrating along hypautomorph amphibole (magnesiohornblende) grains (Amp) and plagioclase of andesite to labradorite composition (Plg) in the biotite gabbro M-5-3 from Mařiz. Numerous apatite (Ap) grains are present. **D** — An elongated hypautomorph laths of ilmenite (Ilm) with isometric titanite (Ttn) at the contact with pargasite (Amp) and plagioclase (Plg) of andesine to labradorite composition. Note the unusual parallel structure of the Mešovice hornblende norite.

Table 3: Representative microprobe analyses of olivine and empirical formulae based on 4 oxygens.

stantial amounts also occur in the Mařiz olivine gabbro (M-5-1), gabbro (M-5-2) and gabbro (M-5-3). Clinopyroxene is present as euhedral to subhedral crystals while smaller subhedral grains occur in the matrix. All the clinopyroxenes have the composition of diopside (Table 4 and Fig. 3 — Morimoto 1988 classification), with compositions in the range of $En_{45-37}Fs_{15-07}Wo_{53-46}$. The clinopyroxene crystals are largely homogeneous but with indistinct chemical and coloured zoning (light brown to light green).

Amphiboles are, together with orthopyroxenes the most abundant ferromagnesian minerals of the gabbroic rocks. They are either primary, represented by minor dark brown and deep green subhedral crystals or secondary pale green acicular

Sample Analysis	M-1b COR/C	M-1b COR/C	M-2 COR/C	M-5-1 C	M-5-1 R
Location	Nonndorf		Korolupy	Mařiz	
SiO ₂	36.86	36.41	36.57	39.40	39.27
TiO ₂	0.00	0.06	0.00	0.00	0.00
FeO	34.78	37.89	33.91	23.23	23.64
MnO	0.33	0.53	0.38	0.26	0.26
MgO	27.96	25.28	28.72	37.15	36.49
CaO	0.00	0.00	0.04	0.00	0.04
Total	99.93	100.17	99.62	100.04	99.70
Si	1.018	1.020	1.011	1.024	1.027
Ti	0.000	0.001	0.000	0.000	0.000
Fe ²⁺	0.804	0.888	0.784	0.505	0.517
Mn	0.008	0.013	0.009	0.006	0.006
Mg	1.151	1.056	1.184	1.439	1.422
Ca	0.000	0.000	0.001	0.000	0.001
Cations	2.981	2.978	2.989	2.974	2.989
Mg/(Fe+Mg)	0.59	0.54	0.60	0.74	0.73

C — core, R — rim, COR — coronite structure

Table 4: Representative microprobe analyses of orthopyroxene and clinopyroxene and empirical formulae based on 4 cations.

Sample Analysis Location	M-1b COR/C Nonndorf		M-1b COR/I Nonndorf		M-1b COR/II Nonndorf		M-2 COR/C Korolupy		M-2 COR/R Korolupy		M-5-1 C-R	M-5-2 C Maříž		M-5-2 R Maříž		M-5-2 IG (amp)	M-3A C Uherčice		M-3A R Uherčice		M-3B Ph/C	M-3B Ph/R	M-5-2 IG (amp)	M-5-3 C Maříž	M-5-3 R
	4	4	4	4	4	4	4	4	4	4	4	4	4	4	4	4	4	4	4	4	4	4	4	4	4
SiO ₂	54.07	52.46	50.48	54.54	53.38	55.10	53.85	53.79	55.91	53.68	53.38	53.85	53.79	55.91	53.68	53.92	53.78	54.09	51.71	51.71	51.71	53.92	53.78	53.71	
TiO ₂	0.00	0.00	0.08	0.02	0.00	0.10	0.17	0.22	0.10	0.12	0.13	0.17	0.22	0.10	0.12	0.16	0.16	0.04	0.54	0.54	0.54	0.16	0.16	0.00	
Al ₂ O ₃	0.84	1.53	1.33	0.49	0.90	2.88	3.88	3.16	0.85	1.24	1.11	3.88	3.16	0.85	1.24	1.60	0.97	0.45	3.26	3.26	3.26	1.60	0.97	0.79	
Cr ₂ O ₃	0.03	0.00	0.07	0.00	0.00	0.02	0.75	0.27	0.04	0.00	0.02	0.75	0.27	0.04	0.00	0.42	0.04	0.25	0.00	0.00	0.42	0.04	0.03		
FeO	21.62	25.00	31.89	19.90	22.49	13.73	11.39	13.32	14.53	19.90	5.77	11.39	13.32	14.53	5.38	4.15	8.08	4.94	7.00	7.00	7.00	4.15	8.08	8.22	
MnO	0.42	0.53	0.65	0.31	0.45	0.17	0.23	0.30	0.33	0.33	0.33	0.23	0.30	0.33	0.18	0.22	0.30	0.33	0.39	0.39	0.39	0.22	0.30	0.37	
MgO	22.82	20.17	15.28	23.95	21.55	27.67	27.66	26.52	27.81	21.55	13.69	27.66	26.52	27.81	14.28	15.88	14.29	14.62	12.56	12.56	12.56	15.88	14.29	12.41	
CaO	0.32	0.25	0.29	0.12	0.26	0.28	1.58	1.88	0.37	0.26	24.02	1.58	1.88	0.37	23.98	23.79	22.92	23.75	23.46	23.46	23.79	22.92	24.66		
Na ₂ O	0.00	0.00	0.00	0.00	0.00	0.00	0.00	0.00	0.00	0.00	0.18	0.00	0.00	0.00	0.23	0.23	0.21	0.21	0.25	0.25	0.23	0.21	0.25		
Total	100.12	99.94	100.07	99.33	99.03	99.95	99.51	99.46	99.94	98.61	98.61	99.51	99.46	99.94	99.09	100.37	100.75	98.68	99.17	99.17	100.37	100.75	100.44		
T Si	2.005	1.980	1.970	2.022	2.013	1.972	1.925	1.938	2.009	2.007	2.007	1.925	1.938	2.009	2.001	1.969	1.985	2.024	1.942	1.942	1.969	1.985	2.003		
T Al	0.000	0.020	0.030	0.000	0.000	0.028	0.075	0.062	0.000	0.000	0.000	0.075	0.062	0.000	0.000	0.031	0.015	0.000	0.058	0.058	0.031	0.015	0.000		
M1 Al	0.037	0.048	0.032	0.021	0.040	0.093	0.089	0.072	0.036	0.049	0.049	0.089	0.072	0.036	0.054	0.038	0.028	0.020	0.087	0.087	0.038	0.028	0.035		
M1 Ti	0.000	0.000	0.002	0.001	0.000	0.003	0.005	0.006	0.003	0.004	0.004	0.005	0.006	0.003	0.003	0.004	0.004	0.001	0.015	0.015	0.004	0.004	0.000		
M1 Fe ²⁺	0.000	0.000	0.075	0.000	0.000	0.000	0.000	0.000	0.000	0.180	0.180	0.000	0.000	0.000	0.148	0.081	0.180	0.155	0.195	0.195	0.081	0.180	0.256		
M1 Cr	0.001	0.000	0.002	0.000	0.000	0.001	0.001	0.008	0.001	0.000	0.000	0.001	0.008	0.001	0.000	0.012	0.001	0.007	0.000	0.000	0.012	0.001	0.001		
M1 Mg	0.962	0.952	0.889	0.978	0.960	0.903	0.885	0.914	0.960	0.767	0.767	0.885	0.914	0.960	0.793	0.865	0.786	0.815	0.703	0.703	0.865	0.786	0.690		
M2 Mg	0.299	0.183	0.000	0.346	0.252	0.573	0.591	0.516	0.530	0.000	0.000	0.591	0.516	0.530	0.000	0.000	0.000	0.000	0.000	0.000	0.000	0.000	0.000		
M2 Fe ²⁺	0.670	0.789	0.966	0.617	0.709	0.411	0.341	0.401	0.437	0.001	0.001	0.341	0.401	0.437	0.019	0.046	0.069	0.000	0.025	0.025	0.046	0.069	0.000		
M2 Mn	0.013	0.017	0.021	0.010	0.014	0.005	0.007	0.009	0.010	0.011	0.011	0.007	0.009	0.010	0.006	0.007	0.009	0.010	0.012	0.012	0.007	0.009	0.012		
M2 Ca	0.013	0.010	0.012	0.005	0.011	0.011	0.061	0.073	0.014	0.968	0.968	0.061	0.073	0.014	0.958	0.931	0.907	0.952	0.944	0.944	0.931	0.907	0.985		
M2 Na	0.000	0.000	0.000	0.000	0.000	0.000	0.000	0.000	0.000	0.013	0.013	0.000	0.000	0.000	0.017	0.016	0.015	0.015	0.018	0.018	0.016	0.015	0.018		
Sum cat	4	4	4	4	4	4	4	4	4	4	4	4	4	4	4	4	4	4	4	4	4	4	4	4	
Wolastonite	0.6	0.5	0.6	0.2	0.5	0.6	3.4	4.3	0.7	50.2	50.2	3.4	4.3	0.7	49.8	48.3	46.4	49.3	50.2	50.2	48.3	46.4	50.7		
Enstatite	64.4	58.2	45.3	67.7	62.3	77.6	78.3	74.7	76.4	39.8	39.8	78.3	74.7	76.4	41.2	44.8	40.3	42.2	37.4	37.4	44.8	40.3	35.5		
Ferrosillite	34.9	41.3	54.1	32.1	37.2	21.9	18.5	21.5	22.9	10.0	10.0	18.5	21.5	22.9	9.0	6.9	13.3	8.5	12.4	12.4	6.9	13.3	13.8		
Jadeite	0.0	0.0	0.0	0.0	0.0	0.0	0.0	0.0	0.0	1.3	1.3	0.0	0.0	0.0	1.7	1.7	1.5	1.6	1.9	1.9	1.7	1.5	1.8		

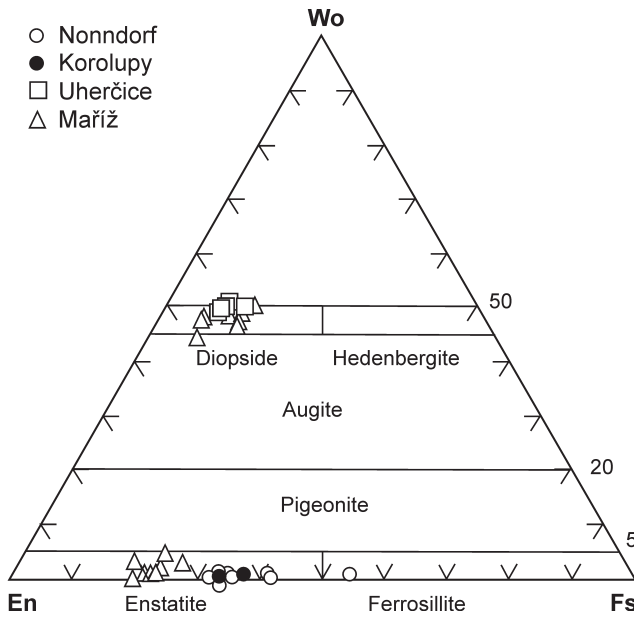
C — core, R — rim, Ph — phenocryst, IG — intergrowth, COR — coronite structure

or prismatic crystals pseudomorphing primary pyroxenes and/or amphiboles. The most abundant primary amphibole variety is pargasite to ferropargasite concentrated in rims of coronitic textures (Fig. 2A,B) of norites from Korolupy and Nonndorf. However, anhedral grains of dark brown pargasite sometimes replace orthopyroxene. The pargasite to ferropargasite (Table 5 and Fig. 4 — Leake (Ed.) 1997 classification) are typical of the Mešovice samples while pargasite to edenite characterize the more strongly amphibolized Uherčice and Maříž gabbroic rocks. Hornblends of the tschermakite to magnesiohornblende series, transitional to the secondary amphiboles, are found in the Maříž rocks in strongly retrogressed metagabbros to well equilibrated gabbroamphibolites. The typical secondary amphiboles have actinolitic compositions. Cummingtonite (mostly after orthopyroxenes) often occurs in the parallel growths with actinolite.

Dark mica is typically rare (~1 vol. %) as anhedral intercumulus crystals in most of the gabbroic rocks but forms up to 35 vol. % in the Maříž gabbro (M-5-3). It penetrates as a younger mineral along the grain boundaries (see Fig. 2C). An $Al^{[6]}$ vs. $Fe_{tot}/(Fe_{tot}+Mg)$ plot (Fig. 5; Fleet 2003) shows the range from phlogopite (Maříž) to biotite in the Korolupy and Nonndorf samples (cf. in Table 6).

Plagioclase is the most abundant component of the gabbroic rocks ranging from subhedral laths to rare euhedral crystals. Its composition varies from anorthite to oligoclase in rims ($An_{20-90}Or_{05-07}Ab_{10-80}$) (cf. Table 7 and Fig. 6). The most calcic feldspars occur in the Uherčice melagabbro whereas oligoclase compositions are associated with samples with uraltized pyroxenes (cf. Koller 1998). **Alkali feldspar** occurs as subhedral grains in some gabbroic samples of the Maříž body with a composition similar to that in the Čiměř muscovite biotite granite (cf. Table 7 and Fig. 6).

Hercynite is present in coronitic assemblages in the Korolupy and Nonndorf norites. Inclusions in the Nonndorf olivines are **Cr-spinels**, whereas inclusions in orthopyroxenes are of magnetite composition. **Magnetite** occurs as rare euhedral to subhedral corroded crystals, generally in association with the mafic minerals and their secondary products.



▲ Fig. 3. Pyroxenes in quadrilateral diagram of Morimoto (1988).

▶ Fig. 4. A, B — Amphiboles in classification diagram of Leake (Ed.) (1997).

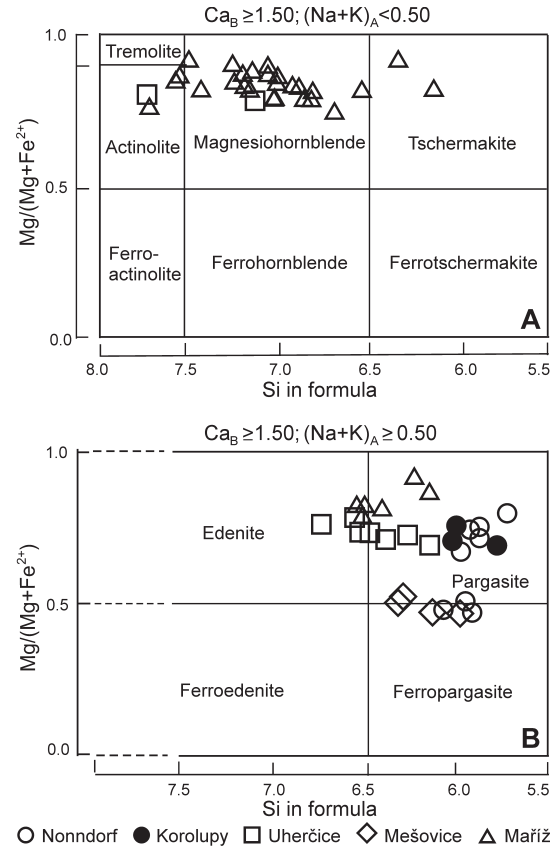


Table 5: Representative microprobe analyses of amphibole and empirical formulae based on 15 cations.

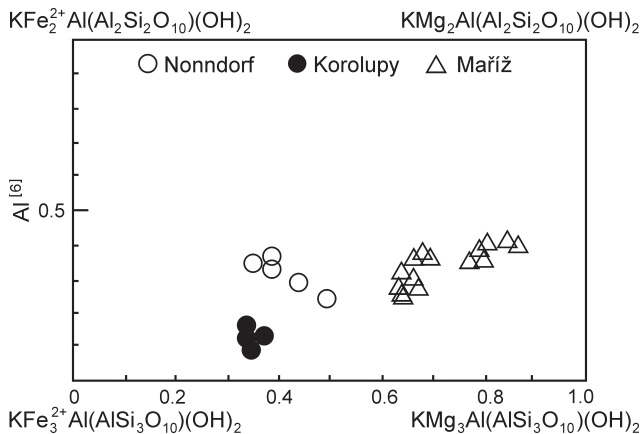
Sample Analysis Location	M-1b COR/C Nonndorf	M-1b COR/R Korolupy	M-2 COR/C Korolupy	M-2 COR/R Korolupy	M-3B Ph/C Uherčice	M-3B Ph/R Uherčice	M-4 Ph/C Mešovice	M-4 Ph/R Mešovice	M-5-2 Ph/C Maříž	M-5-4 C-R/Gr Maříž	M-5-5 C/Br Maříž	M-5-5 R/Gr Maříž
SiO ₂	41.12	41.08	41.58	40.12	45.41	41.76	42.32	39.65	51.36	45.64	50.88	54.87
TiO ₂	0.04	0.07	0.07	0.04	0.19	0.68	1.45	1.60	0.94	1.30	0.12	0.14
Al ₂ O ₃	17.51	18.39	16.72	18.60	12.49	14.54	11.31	14.19	7.48	13.06	7.99	3.97
Cr ₂ O ₃	0.05	0.08	0.00	0.00	0.00	0.64	0.00	0.00	0.83	0.61	0.03	0.00
FeO	10.58	11.06	11.92	12.97	8.62	10.26	18.15	18.44	5.88	5.21	9.28	7.99
MnO	0.18	0.03	0.20	0.12	0.30	0.30	0.20	0.14	0.14	0.11	0.23	0.26
MgO	12.52	12.23	11.95	11.17	14.45	12.34	9.50	8.21	18.93	17.07	17.09	18.71
CaO	11.50	11.44	11.16	10.90	11.68	11.94	11.75	11.54	11.87	11.85	10.81	11.60
Na ₂ O	2.59	2.77	2.36	2.54	2.16	2.52	1.89	2.30	1.13	2.01	1.05	0.51
K ₂ O	0.59	0.73	0.58	0.72	0.29	0.73	0.76	0.91	0.24	0.39	0.20	0.05
Total	96.68	97.88	96.54	97.18	95.59	95.71	97.33	96.98	98.80	97.25	97.68	98.10
T Si	6.017	5.957	6.108	5.878	6.653	6.250	6.401	6.063	7.105	6.469	7.144	7.627
T Al	1.983	2.043	1.892	2.122	1.347	1.750	1.599	1.937	0.895	1.531	0.856	0.373
Sum T	8	8	8	8	8	8	8	8	8	8	8	8
C Al	1.034	1.098	1.000	1.087	0.808	0.812	0.416	0.619	0.324	0.649	0.466	0.277
C Cr	0.006	0.009	0.000	0.000	0.000	0.076	0.000	0.000	0.091	0.068	0.003	0.000
C Fe ³⁺	0.311	0.303	0.376	0.476	0.141	0.035	0.254	0.207	0.295	0.228	0.522	0.328
C Ti	0.004	0.008	0.008	0.004	0.021	0.077	0.165	0.184	0.098	0.139	0.013	0.015
C Mg	2.731	2.644	2.617	2.440	3.156	2.753	2.142	1.872	3.904	3.607	3.577	3.877
C Fe ²⁺	0.903	0.936	0.987	0.985	0.856	1.228	2.010	2.110	0.281	0.303	0.406	0.489
C Mn	0.011	0.002	0.012	0.007	0.019	0.019	0.013	0.009	0.008	0.007	0.013	0.015
Sum C	5	5	5	5	5	5	5	5	5	5	5	5
B Fe ²⁺	0.081	0.102	0.102	0.128	0.059	0.021	0.032	0.042	0.104	0.087	0.162	0.112
B Mn	0.011	0.002	0.013	0.008	0.019	0.019	0.013	0.009	0.008	0.007	0.014	0.015
B Ca	1.803	1.778	1.756	1.711	1.833	1.915	1.904	1.891	1.759	1.800	1.683	1.805
B Na	0.105	0.118	0.129	0.153	0.089	0.046	0.051	0.058	0.128	0.107	0.141	0.068
Sum B	2	2	2	2	2	2	2	2	2	2	2	2
A Na	0.630	0.661	0.543	0.568	0.525	0.686	0.503	0.624	0.175	0.446	0.088	0.000
A K	0.110	0.135	0.109	0.135	0.054	0.139	0.147	0.178	0.042	0.071	0.036	0.007
Sum A	0.740	0.796	0.651	0.703	0.579	0.825	0.650	0.801	0.218	0.516	0.124	0.002
Sum_cat	15.740	15.796	15.651	15.703	15.579	15.825	15.650	15.801	15.218	15.516	15.124	15.002
Sum_ox	23.006	23.030	23.011	23.000	23.067	23.053	23.000	23.000	23.050	23.050	23.043	23.059

C — core, R — rim, Ph — phenocryst, IG — intergrowth, COR — coronite structure, Br — brown, Gr — green

Table 6: Representative microprobe analyses of mica and empirical formulae based on 22 oxygens.

Sample Analysis Location	M-1b R Nonndorf	M-1b R Nonndorf	M-2 C Korolupy	M-2 R Korolupy	M-5-1 C Maříž	M-5-3 IG (cpx) Maříž	M-5-5 Ph/C Maříž
SiO ₂	35.08	35.49	34.84	35.35	38.74	37.45	37.53
TiO ₂	5.90	4.02	5.03	5.65	3.16	3.43	3.15
Al ₂ O ₃	14.31	15.89	14.22	13.71	16.37	15.24	15.82
Cr ₂ O ₃	0.03	0.06	0.00	0.00	0.50	0.18	0.20
FeO	24.12	19.83	24.45	24.25	8.06	14.11	13.12
MnO	0.02	0.09	0.00	0.00	0.00	0.21	0.11
MgO	7.39	11.18	7.08	6.47	18.41	14.26	15.26
BaO	0.06	0.00	0.00	0.03	0.25	0.77	0.29
Na ₂ O	0.15	0.35	0.01	0.00	0.65	0.09	0.13
K ₂ O	9.44	8.88	9.26	9.31	8.37	9.64	8.99
Total	96.50	95.79	94.89	94.77	94.51	95.38	94.60
Si	5.444	5.402	5.502	5.581	5.605	5.603	5.586
Al ^{IV}	2.556	2.598	2.498	2.419	2.395	2.397	2.414
Al ^{VI}	0.059	0.250	0.147	0.130	0.394	0.288	0.359
Ti	0.689	0.460	0.598	0.671	0.344	0.386	0.353
Fe ²⁺	3.130	2.524	3.229	3.202	0.975	1.765	1.633
Cr	0.004	0.007	0.000	0.000	0.057	0.021	0.024
Mn	0.003	0.012	0.000	0.000	0.000	0.027	0.014
Mg	1.710	2.537	1.667	1.523	3.971	3.180	3.386
Ba	0.004	0.000	0.000	0.002	0.014	0.045	0.017
Na	0.045	0.103	0.003	0.000	0.182	0.026	0.038
K	1.869	1.725	1.866	1.875	1.545	1.840	1.707
Cations	15.513	15.618	15.510	15.403	15.482	15.578	15.531
Mg/(Fe+Mg)	0.35	0.50	0.34	0.32	0.80	0.64	0.67

C — core, R — rim, IG — intergrowth, Ph — phenocryst

**Fig. 5.** Dark micas in 100 Fe_{tot}/(Fe_{tot}+Mg) vs. Al^{VI} diagram after Fleet (2003).

The highest concentrations are in the Maříž (M-5-4) and Mešovice samples. The compositions show very low ulvöspinel contents (Usp 0–4 mol %). **Ilmenite** is present as a decomposition product of the primary titanium-rich magnetite from Korolupy, and Maříž (together with rare **rutile**) or penetrates as a younger mineral along grain boundaries (Mešovice, MnO ~ 10 wt. %, Fig. 2D) where it is partly “leucoxenized” and transformed to titanite. Small crystals of **titanite** occur in association with ilmenite in all gabbroic rocks. However, subhedral grains of **almandine**, in symplectite association with ilmenite occur in norite from Korolupy and as individual isometric grains in melanorite from Uherčice. **Pyrrhotite** has been found at Maříž only. **Fluorapatite** occurs in all the gab-

broic rocks but **zircon** is known only as a scarce accessory mineral in Maříž. **Pyrite** is present in all the gabbroic rocks, particularly at Mešovice where it occurs with **chalcopyrite**.

Geothermobarometry

Temperature and pressure estimates are difficult to obtain as a result of compositional variability in the minerals arising from recrystallization and partial re-equilibration during cooling and decompression. Estimates of the highest temperature and pressure equilibration conditions of the rocks are therefore based on the core compositions of minerals judged, on textural grounds, to represent the earliest assemblages.

Temperatures were calculated using the plagioclase-amphibole thermometer of Holland & Blundy (1994). Additionally, in samples with coronitic texture (Korolupy and Nonndorf), the temperature of coronas was calculated using “Ca-in-orthopyroxene thermometer” of Brey & Köhler

(1990). Because of the lack of a precise barometer for clinopyroxene-free gabbroic rocks, pressures were calculated only for clinopyroxene-bearing gabbros using the clinopyroxene geobarometer (Nimis 1999). The BH model of Nimis (1999) was selected as the most reliable, because it is calibrated for a composition similar to that of the gabbros under consideration.

Equilibrium temperature and pressure estimates are given in Table 8. The temperatures calculated for pressures 5–10 kbar are similar for coronitic (700–840 °C) and non-coronitic gabbroic rocks (680–850 °C). The pressures calculated for the Uherčice melanorite and Maříž gabbro (M-5-3) range from 7 to 13 kbar. This large uncertainty reflects the strong dependence of the clinopyroxene barometer on the estimated temperature. The two-pyroxene thermometry (1000–700 °C) and clinopyroxene-plagioclase barometry (8–5 kbar) performed by Koller (1998) also show a wide scatter of data for these rocks.

Geochemical characteristics of the gabbroic rocks

Major element and trace element data of ten gabbroic rock samples from one locality in the Moldanubian Monotonous Unit and four localities from the Vratěnín Unit of the Moravian affinity, and one granite sample from the Moldanubian pluton are presented in Table 9.

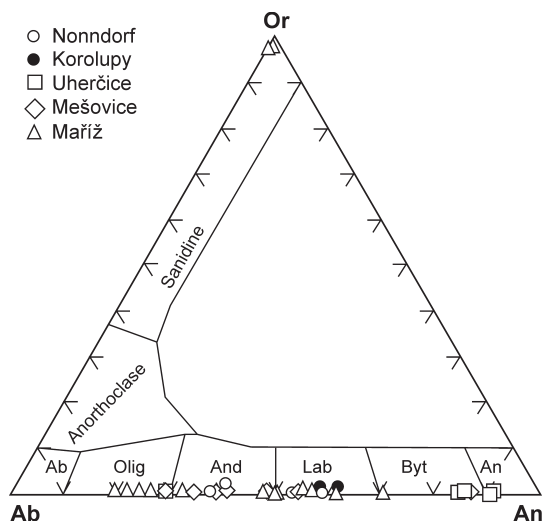
Major and minor elements

The gabbroic rocks show large variation of Mg# from 61 (49) to 83 [Mg# = 100Mg/(Mg+Fe²⁺) for Fe³⁺/Fe=0.15]. The

Table 7: Representative microprobe analyses of feldspars and empirical formulae based on 32 oxygens.

Sample Analysis Location	M-1b COR/C Nonndorf	M-1b COR/R	M-2 Ph/C Korolupy	M-2 Ph/R	M-3B Ph/C Uherčice	M-3B Ph/R	M-4 INC/C Mešovice	M-4 INC/R	M-5-3 Ph/C	M-5-3 Ph/R	M-5-5 Ph/R	M-5-5 Ph
SiO ₂	53.14	57.79	53.15	54.81	45.24	60.85	46.00	60.52	50.45	55.62	64.00	64.61
TiO ₂	0.00	0.06	0.03	0.00	0.00	0.04	0.00	0.00	0.00	0.03	0.00	0.00
Al ₂ O ₃	30.57	26.85	29.68	29.37	34.88	24.70	35.02	25.35	31.83	28.58	23.31	18.51
FeO	0.14	0.19	0.29	0.19	0.10	0.13	0.37	0.27	0.02	0.07	0.00	0.02
MnO	0.02	0.03	0.03	0.00	0.00	0.00	0.02	0.00	0.00	0.00	0.00	0.00
MgO	0.01	0.01	0.26	0.12	0.00	0.00	0.01	0.00	0.00	0.00	0.00	0.00
BaO	0.00	0.00	0.00	0.00	0.00	0.00	0.00	0.00	0.00	0.03	0.03	0.19
CaO	12.26	8.08	12.37	11.01	18.38	6.19	17.48	6.14	14.56	10.04	4.14	0.00
Na ₂ O	4.70	7.34	4.45	5.21	0.94	8.15	1.43	8.16	3.37	5.52	9.42	0.20
K ₂ O	0.04	0.06	0.05	0.05	0.00	0.03	0.00	0.10	0.05	0.15	0.13	16.50
Total	100.88	100.41	100.31	100.76	99.54	100.09	100.33	100.54	100.28	100.04	101.03	100.03
Si	9.541	10.322	9.605	9.809	8.375	10.812	8.441	10.721	9.168	9.994	11.199	11.968
Al	6.464	5.648	6.316	6.190	7.605	5.168	7.568	5.288	6.812	6.048	4.803	4.038
Ti	0.000	0.008	0.004	0.003	0.000	0.005	0.000	0.000	0.000	0.004	0.000	0.000
Fe ²⁺	0.021	0.028	0.044	0.028	0.015	0.019	0.057	0.040	0.003	0.011	0.000	0.003
Mn	0.003	0.005	0.005	0.000	0.000	0.000	0.003	0.000	0.000	0.000	0.000	0.000
Mg	0.003	0.003	0.070	0.032	0.000	0.000	0.003	0.000	0.000	0.000	0.000	0.000
Ba	0.000	0.000	0.000	0.000	0.000	0.000	0.000	0.000	0.000	0.002	0.002	0.014
Ca	2.358	1.546	2.395	2.111	3.646	1.178	3.437	1.165	2.835	1.933	0.776	0.000
Na	1.636	2.542	1.559	1.808	0.337	2.808	0.509	2.803	1.187	1.923	3.196	0.072
K	0.009	0.014	0.012	0.011	0.000	0.007	0.000	0.023	0.012	0.034	0.029	3.899
Z	16.005	15.978	15.925	16.000	15.980	15.985	16.009	16.009	15.980	16.046	16.002	16.006
X	4.030	4.138	4.085	3.990	3.998	4.012	4.009	4.031	4.037	3.903	4.003	3.988
Albite	40.9	62.0	39.3	46.0	8.5	70.3	12.9	70.2	29.4	49.4	79.8	1.8
Anorthite	58.9	37.7	60.4	53.7	91.5	29.5	87.1	29.2	70.3	49.7	19.4	0.0
Orthoclase	0.2	0.3	0.3	0.3	0.1	0.2	0.1	0.6	0.3	0.9	0.7	97.8
Celsian	0.0	0.0	0.0	0.0	0.0	0.0	0.0	0.0	0.0	0.1	0.1	0.4

C — core, R — rim, Ph — phenocryst, INC — inclusion, COR — coronite structure

**Fig. 6.** Feldspars in Ab-Or-An diagram after Smith (1974).

lower Mg# (61–64) are typical for coronitic norites from Korolupy and Nonndorf. Only the Mešovice norite has a lower Mg# of 49 coupled with high TiO₂ contents (3.4 wt. %), higher contents of Fe₂O₃, P₂O₅ together with Zr, and very low contents of compatible elements (Cr, Co), showing a more fractionated nature of the rocks after earlier accumulation of Mg-bearing phases. The relationship between the SiO₂ and alkalis of the studied rocks is illustrated on TAS diagram (Fig. 7; Cox et al. 1979). In spite of their similar petrography, the two samples from Maříž (M-5-2 and M-5-4) straddle the gabbro field boundary towards the lower alkali contents. No significant correlations were found between SiO₂ and selected oxides (Al₂O₃, MgO, TiO₂, P₂O₅, see Fig. 8). The wide variability of compatible element contents, for example Ni (53–1076 ppm), Co (16–140 ppm), Cr (22–1867 ppm), V (159–521 ppm), and Sc (22–40 ppm) and Sr-Nd isotopes illustrates the heterogeneity of the gabbroic rocks even from a single locality, such as Maříž.

Table 8: Estimated equilibration temperatures and pressures of the gabbroic rocks.

Locality/No.	Rock type	Temperature (°C)		Pressure (kbar)
		Plg-Amp	Ca-in-opx*	Cpx (BH model)
Nonndorf (M-1b)	Olivine norite (coronitic)	700–840	670–800	
Korolupy (M-2)	Norite (coronitic)	710–810	640–770	
Uherčice (M-3A)	Amphibole melanorite	780–850		7–12
Mešovice (M-4)	Hornblende norite	740–850		
Maříž (M-5-1)	Hornblende ol. gabbro	810–860		
Maříž (M-5-3)	Biotite gabbro	680–720		8–13

*temperature estimates for olivine-orthopyroxene-amphibole coronas. Plg-Amp—plagioclase — amphibole thermometer of Holland & Blundy (1994) calculated for pressures from 5 to 10 kbar; Ca-in-opx — orthopyroxene thermometer of Brey & Köhler (1990) calculated for pressures 5–10 kbar; Cpx (BH model) — clinopyroxene barometer (BH model) of Nimis (1999) calculated for temperatures obtained from Plg-Amp thermometer.

Table 9: Chemical composition of the gabbroic rocks.

Sample	M/1b	M-2	M-3A	M-3B	M-4	M-5-1	M-5-2	M-5-3	M-5-4	M-5-5	M-6
SiO ₂	49.12	50.48	46.14	46.52	41.68	49.86	51.72	45.26	47.22	49.96	73.08
TiO ₂	0.98	0.95	0.91	0.56	3.38	0.44	0.37	1.68	0.28	1.00	0.23
Al ₂ O ₃	15.75	15.86	14.88	12.84	14.21	15.32	10.26	14.78	4.15	18.47	14.33
Fe ₂ O ₃	1.95	1.91	1.30	1.95	4.70	0.89	1.40	1.67	3.05	1.69	0.44
FeO	8.86	8.18	4.30	5.41	11.53	6.55	7.01	7.22	9.48	4.14	0.99
MnO	0.15	0.14	0.19	0.21	0.16	0.12	0.15	0.12	0.18	0.13	0.02
MgO	8.98	7.38	9.77	11.13	7.29	13.77	18.46	10.95	27.62	8.18	0.36
CaO	9.06	9.92	16.69	16.82	11.60	8.97	7.68	9.58	2.41	8.75	0.79
Na ₂ O	2.66	2.87	1.04	1.08	1.95	1.51	0.95	1.16	0.25	2.25	2.91
K ₂ O	0.38	0.40	1.54	1.05	0.73	0.36	0.26	3.48	0.09	1.97	5.32
P ₂ O ₅	0.15	0.15	0.13	0.09	0.25	0.08	0.07	1.06	0.10	0.10	0.25
H ₂ O ⁻	0.10	0.14	0.20	0.18	0.16	0.18	0.18	0.14	0.10	0.24	0.04
H ₂ O ⁺	0.83	0.76	1.98	1.44	1.89	0.67	0.77	2.09	4.00	2.50	0.66
CO ₂	0.48	0.47	0.41	0.30	0.16	0.70	0.35	0.24	0.58	0.24	0.15
Total	99.45	99.61	99.48	99.58	99.69	99.42	99.63	99.43	99.51	99.62	99.57
Rb (ppm)	9.56	8.75	48.99	29.46	15.64	12.18	6.60	151.80	2.71	130.6	310.0
Cs	0.52	0.39	2.30	1.68	0.45	3.73	1.46	13.66	1.62	8.86	17.78
Sr	203	240	231	212	498	415	207	1273	51	584	64
Ba	94	149	412	233	215	150	89	3961	51	622	253
Pb	1.92	0.90	25.58	5.59	7.62	2.61	2.61	7.03	1.83	14.32	29.43
Sc	21.4	22.0	31.0	32.4	35.1	28.6	39.8	33.8	28.2	26.0	2.7
Y	12.2	11.4	14.3	9.1	15.6	7.2	6.7	14.9	4.2	19.1	8.1
La	5.02	5.01	11.26	4.83	14.16	4.04	2.53	69.15	2.10	9.24	23.63
Ce	11.54	11.53	25.52	11.01	31.94	8.84	5.72	153.10	4.72	20.98	52.90
Pr	1.64	1.62	3.44	1.53	4.34	1.17	0.79	20.27	0.62	2.72	6.68
Nd	7.15	7.74	13.45	6.47	18.47	5.12	3.50	79.27	2.65	11.56	24.45
Sm	2.10	2.24	3.12	1.73	4.55	1.20	0.93	10.97	0.58	2.89	5.40
Eu	0.91	0.99	1.09	0.72	1.64	0.65	0.40	3.51	0.21	1.23	0.51
Gd	2.37	2.44	2.81	1.77	4.10	1.26	1.00	6.12	0.59	3.24	3.73
Tb	0.40	0.41	0.48	0.29	0.63	0.20	0.18	0.81	0.11	0.54	0.51
Dy	2.40	2.27	2.85	1.85	3.43	1.34	1.21	3.40	0.72	3.33	1.98
Ho	0.48	0.43	0.53	0.35	0.64	0.28	0.25	0.58	0.16	0.68	0.28
Er	1.29	1.19	1.49	0.96	1.61	0.81	0.73	1.49	0.48	1.99	0.67
Tm	0.17	0.15	0.21	0.14	0.20	0.11	0.12	0.17	0.08	0.28	0.08
Yb	1.09	0.92	1.25	0.85	1.16	0.76	0.78	0.95	0.52	1.71	0.48
Lu	0.15	0.14	0.18	0.12	0.16	0.11	0.11	0.14	0.09	0.26	0.06
Th	1.23	0.72	4.55	1.02	1.49	0.59	0.54	2.65	0.36	2.48	17.23
U	0.18	0.19	2.23	0.33	0.36	0.15	0.15	0.64	0.11	0.58	8.76
Zr	22.90	18.00	31.6	21.9	32.1	25.6	14.3	15.2	13.2	36.0	85.2
Hf	0.79	0.60	1.33	0.80	1.52	0.75	0.52	0.88	0.40	1.14	2.83
V	182	165	193	192	521	186	245	230	159	139	10.4
Nb	5.06	4.68	7.10	2.93	21.28	1.92	0.85	10.50	0.99	4.00	15.84
Ta	1.58	0.86	0.68	0.58	1.34	0.48	0.27	0.49	0.26	0.51	1.58
Cr	340	224	337	515	22	1242	1867	149	1842	528	6
Co	54	46	16	27	65	54	57	51	140	39	1.7
Ni	167	95	53	133	129	141	149	157	1076	211	2.0
#Mg	64.0	61.0	78.9	76.5	49.3	79.7	82.4	72.5	82.6	75.2	35.3
ΣREE	36.7	37.1	67.7	32.6	87.0	25.9	18.2	349.9	13.6	60.7	121.4
La_N/Yb_N	3.30	3.92	6.44	4.10	8.75	3.80	2.33	52.42	2.90	3.88	35.45
Eu/Eu*	1.24	1.29	1.10	1.24	1.14	1.61	1.26	1.19	1.09	1.22	0.33
La/Nb	0.99	1.07	1.59	1.65	0.67	2.11	2.98	6.59	2.13	2.31	1.49
Nb_N/Th_N	0.49	0.77	0.19	0.34	1.71	0.38	0.19	0.47	0.33	0.19	0.11
Zr_N/Sm_N	0.43	0.32	0.40	0.50	0.28	0.84	0.61	0.06	0.90	0.49	0.62

Trace elements

The chondrite-normalized REE patterns reveal similar trends (cf. Fig. 9A) with characteristic LREE enrichment in most of the samples. Nonetheless, the degree of LREE enrichment is high ($La_N/Yb_N=2.2-49.1$), with the highest degree of REE fractionation observed in the Maříž gabbro sample M-5-2. A distinct positive Eu anomaly present in all the studied samples ($Eu/Eu^*=1.1$ to 1.6) is in agreement with plagioclase accumulations in the studied rocks.

The primitive mantle-normalized incompatible trace element patterns of the gabbroic rocks show differences between both absolute and relative trace element abundances (cf. Fig. 9B). Nevertheless, most of the samples show similar distinctively fractionated patterns with common positive peaks at K and Sr, but negative anomalies for Nb and Zr ($Nb_N/Th_N=0.2-0.8$, $Zr_N/Sm_N=0.1-0.9$). The only exception is in a sample of norite from Mešovice, which is very rich in TiO₂ and Nb (3.4 wt. % and 21.3 ppm, respectively) due to the high modal contents of titanian magnetite, ilmenite (0.1–0.3 wt. % Nb₂O₅), and titanite (0.3–0.9 wt. % Nb₂O₅). The trace element

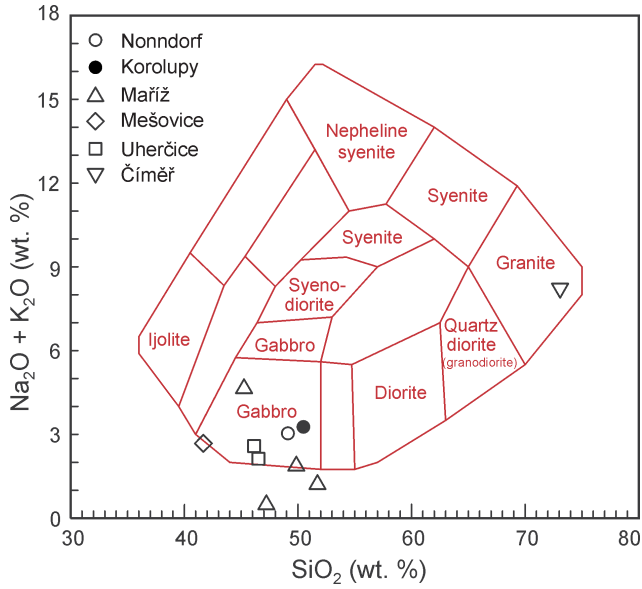


Fig. 7. Total alkali-silica diagram of Cox et al. (1979) showing the composition of the gabbroic rocks.

pattern of the Číměř granite from the Moldanubian pluton differs from those of the gabbroic rocks in its higher Th, K_2O and REE concentrations (Fig. 9A,B) and the presence of the characteristic negative Eu anomaly ($\text{Eu}/\text{Eu}^* = 0.3$).

⁸⁷Sr/⁸⁶Sr and ¹⁴³Nd/¹⁴⁴Nd isotopic systematics

The Nd-Sr isotopic compositions of the gabbroic samples and a single sample of Variscan-age granite associated with the Maříž gabbros are listed in Table 10 and plotted in Fig. 10. As outlined below, K-Ar ages of 570 to 550 Ma for hornblende relics, interpreted to be of magmatic origin, suggest a Cadomian age for these suites. Regression of the Sm-Nd data for all samples, with the exception of the isotopically distinct Uherčice melagabbros, yielded an age of 290 Ma and a large error of ~700 Ma. Rb-Sr isotopic data for these samples yielded 660 Ma and an error of 370 Ma. The Sm-Nd isotopic data from two gabbroic samples from the Uherčice Complex plot on a line corresponding to 1.3 Ga. Clearly the Rb-Sr and Sm-Nd isotopic systems do not help to constrain geologically meaningful ages for these rocks. In the following we accept a crystallization age of 560 Ma for them and outline some source characteristics for these mafic lithologies of the

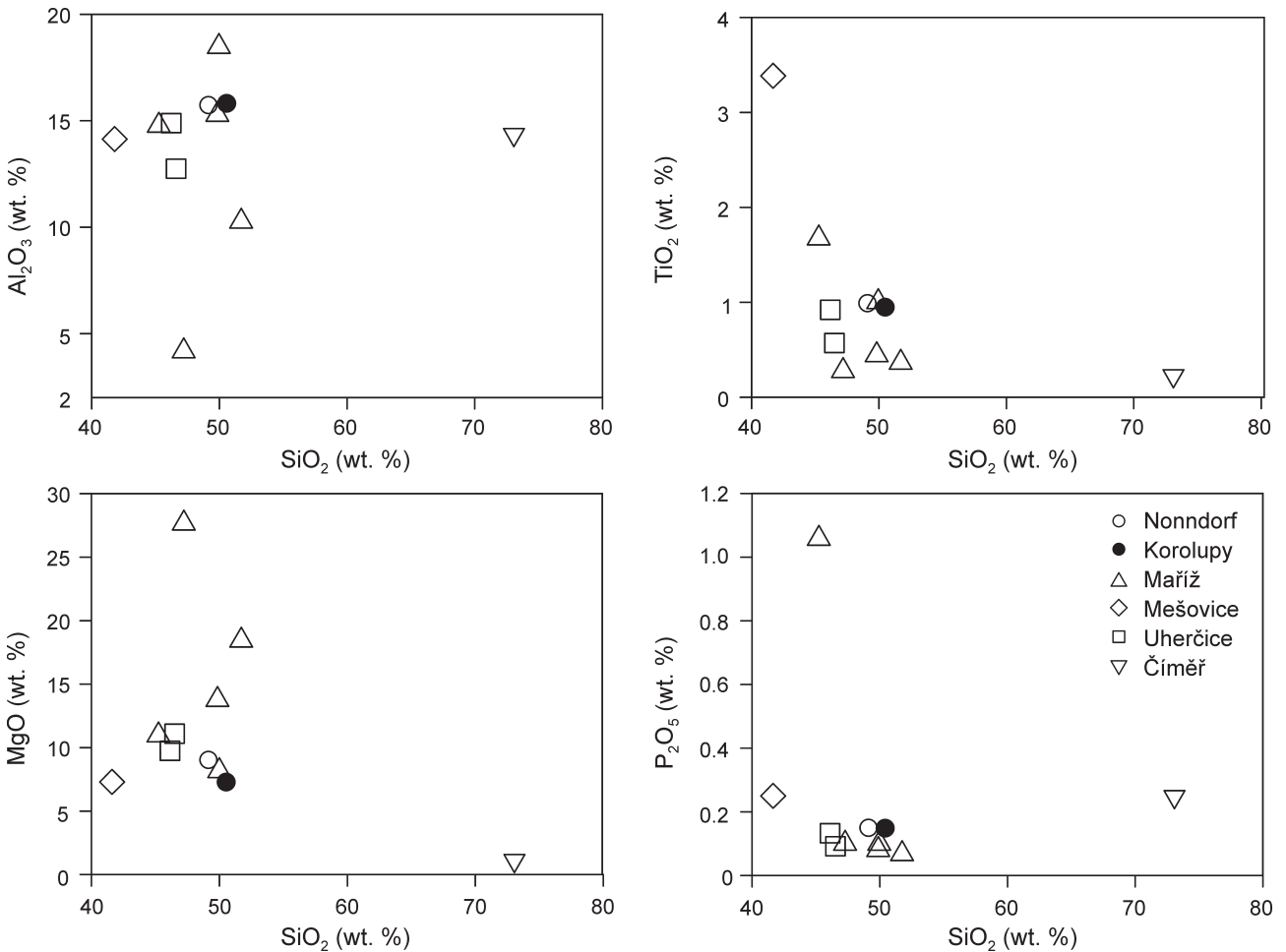


Fig. 8. Harker's diagrams of indicative major and trace element variation of the gabbroic rocks.

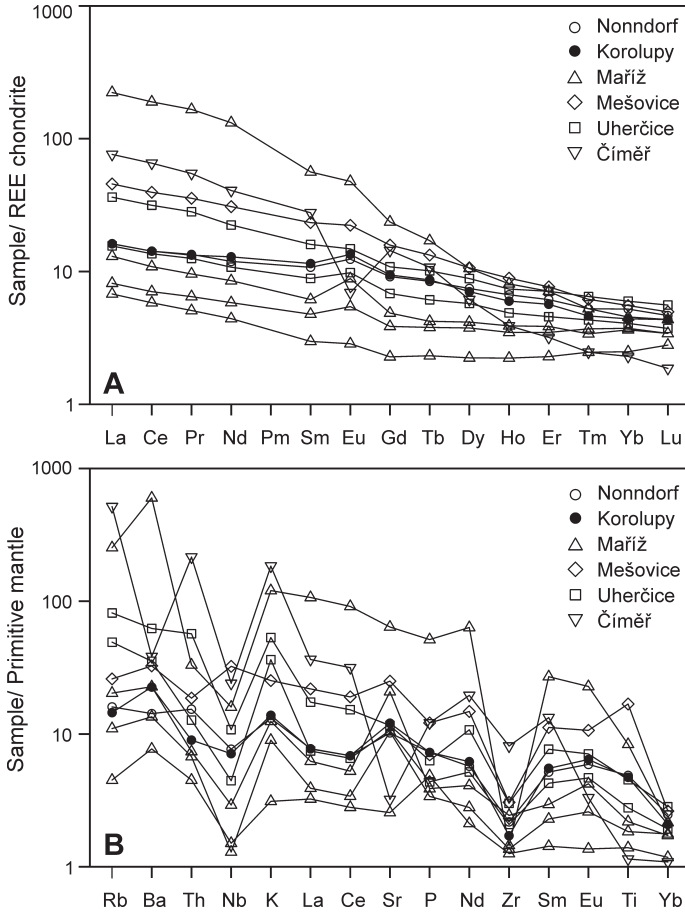


Fig. 9. A — Chondrite-normalized REE patterns for the gabbroic rocks. B — Primitive mantle-normalized incompatible trace element patterns. Normalizing values from Sun & McDonough (1989).

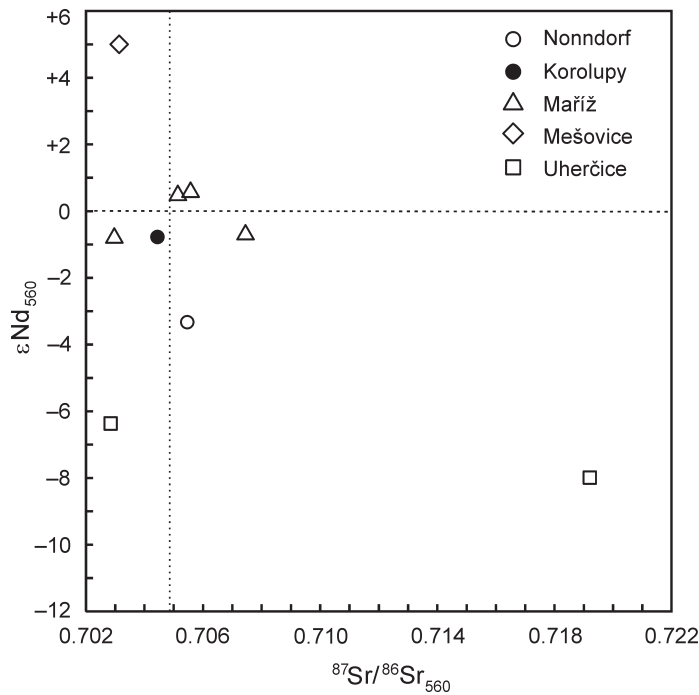


Fig. 10. Initial $^{87}\text{Sr}/^{86}\text{Sr}$ vs. ϵ_{Nd} isotopic ratios for the gabbroic rocks.

Table 10: Rb-Sr and Sm-Nd isotopic data for the gabbroic rocks.

Sample	Rock type	Age (Ma)	Rb ppm	Sr ppm	$^{87}\text{Rb}/^{86}\text{Sr}$	$^{87}\text{Sr}/^{86}\text{Sr}(\text{m})$	$^{87}\text{Sr}/^{86}\text{Sr}(\text{t})$	Nd ppm	Sm ppm	$^{147}\text{Sm}/^{144}\text{Nd}$	$^{149}\text{Nd}/^{144}\text{Nd}(\text{m})$	$^{149}\text{Nd}/^{144}\text{Nd}(\text{t})$	$\epsilon_{\text{Nd}(\text{t})}$
M-1b	Olivine norite	~560	9.6	203	0.140	0.706329 ± 10	0.70523	7.47	2.15	0.1744	0.512379 ± 10	0.511749	-3.3
M-2	Norite	~560	8.7	240	0.110	0.705222 ± 12	0.70436	7.67	2.23	0.1757	0.512518 ± 10	0.511873	-0.8
M-3A	Hbl. melanorite	~560	49.0	231	0.620	0.723949 ± 12	0.71909	13.88	3.05	0.1328	0.511995 ± 10	0.511508	-8.0
M-3B	Hbl. melagabbro	~560	29.5	212	0.403	0.705908 ± 12	0.70275	6.48	1.61	0.1507	0.512146 ± 35	0.511593	-6.3
M-4	Hornblende norite	~560	15.6	498	0.091	0.703757 ± 12	0.70304	19.11	4.48	0.1419	0.512694 ± 09	0.512173	5.0
M-5-1	Hbl. ol. gabbronorite	~560	12.2	415	0.085	0.705788 ± 12	0.70512	4.59	1.08	0.1415	0.512469 ± 10	0.511950	0.6
M-5-2	Gabbronorite	~560	6.6	207	0.092	0.703760 ± 12	0.70304	3.39	0.86	0.1538	0.512445 ± 12	0.511881	-0.7
M-5-3	Biotite gabbro	~560	152	1273	0.345	0.708429 ± 12	0.70572	79.27	10.97	0.0837	0.512259 ± 09	0.511952	0.7
M-5-5	Hornblende gabbro	~560	147	640	0.665	0.709780 ± 12	0.70467	11.41	2.778	0.1472	0.512426 ± 11	0.511886	-0.6
M-6	Two-mica granite	~330	310	64.0	14.100	0.776829 ± 12	0.71049	24.84	5.54	0.1349	0.512165 ± 10	0.512165	-6.6

m — measured ratio, t — initial ratio; $^{87}\text{Sr}/^{86}\text{Sr}$ are normalized to $^{86}\text{Sr}/^{88}\text{Sr} = 0.1194$. Determination of the accuracy and external precision for NIST 987 yielded. $^{87}\text{Sr}/^{86}\text{Sr} = 0.710237 \pm 11$ (N = 18). $^{149}\text{Nd}/^{144}\text{Nd}$ ratios are normalized to $^{146}\text{Nd}/^{144}\text{Nd} = 0.7219$. Error of $^{147}\text{Sm}/^{144}\text{Nd}$ is ~ 0.2% (2σ). An Ames Nd standard solution prepared at Munich yielded: $^{149}\text{Nd}/^{144}\text{Nd} = 0.512095 \pm 12$ (2σ, N = 25); the ratios were corrected for machine bias by adding 0.000040 so that Ames gives a ratio of 0.512135 equivalent to 0.511850 in the La Jolla Nd standard. Sm and Nd determined were determined by isotope dilution. Rb and Sr by ICP-MS.

Moldanubian basement. Because all samples, except those from Nonndorf, have low Sm/Nd ratios, age uncertainties up to 20 Ma will have only negligible effects on the calculated initial ϵ_{Nd} values.

The initial ϵ_{Nd} values calculated for 560 Ma show a very large variation of +5 to -8 (Fig. 10; Table 10). They document a magmatic history of these gabbroic complexes characterized by involvement of juvenile mantle-derived material as seen in the norite sample from Mešovice, and major recycling of ancient crustal components as documented in the Uherčice gabbroic rocks with ϵ_{Nd} values of ca. -6 to -8.

Interpretation of K-Ar ages and fission-track data

The first K-Ar ages on gabbroic rocks from the Moldanubian and Moravian units of W Moravia and N Austria are summarized in Table 11. The majority, measured on amphibole, clinopyroxene, plagioclase and biotite, range from 389 to 254 Ma, confirming the importance of Variscan metamorphic processes on Ar behaviour. However, older ages (1302 Ma and 550 Ma) have been obtained from plagioclase and amphibole at Korolupy, 796 Ma, from plagioclase, from the similar gabbroic body at Nonndorf, and 568 Ma from amphibole at Maříž. It is generally accepted that the closure temperature of amphibole is significantly higher than for plagioclase (Harland et al. 1990), suggesting that the older age of plagioclase is due to excess Ar. This assumption is confirmed by the Variscan age (344 Ma) measured on the plagioclase M-2 at Maříž, after treatment with diluted HF. The plagioclase ages from the gabbroic rocks (M-5-1 and M-5-2) at Maříž are closely similar (389 Ma and 388 Ma), despite the difference in their K contents. This provides an argument against the presence of excess Ar at this locality. K-Ar ages for amphibole and plagioclase from sample M-5-1 correspond to their closure temperatures: the amphibole is significantly older (568 Ma) and is very similar to the age of amphibole from Korolupy sample M-2 (550 Ma), where the excess Ar is indicated by the age of plagioclase. Regarding the importance of Variscan events, the

individual minerals in sample M-2, such as plagioclase (primary and leached), biotite and amphibole of various density fractions, were tested for overprinting, at least partly, during the Variscan events. A separated lower density fraction (partly actinolitized pargasite) yielded a significantly younger age of 449 Ma, while an older age of 573 Ma has been measured on the higher density fraction (pargasite) from M-2.

Since there is no indication from plagioclase of any excess Ar at Maříž, excess Ar is also not inferred for the amphibole. The similarity of amphibole ages at Korolupy (573 Ma) and at Maříž (568 Ma) suggests that Cadomian ages may have been retained during the Variscan tectonometamorphic processes. In units strongly overprinted by the Variscan metamorphism, however, only zircon ages can solve the real age of gabbros.

Apatite fission-track analysis of two gabbroic samples from Korolupy and Maříž (M-5-1) and the Číměř granite indicate very similar ages of 150.2 ± 18.0 Ma (standard deviation $\pm 1\sigma$). Furthermore the samples show comparable track length distribution and shortening of initial fission-track lengths (mean length 11.5 μm) implying a slow and continuous cooling from total annealing zone (i.e. $> 120^\circ\text{C}$) from the Late Jurassic to the present.

Discussion

Rock associations and their relationship

The gabbroic rocks under consideration occur either in the Moldanubian Monotonous Group at contact with the Moldanubian pluton or in the Vratěnín Unit of the Moravian affinity (*sensu* Jenček & Dudek 1971). However, the latter unit was often correlated with the Moldanubian Varied Unit (e.g. Schulmann et al. 2005 and references therein). We prefer to correlate the Vratěnín Group with the Moravian Unit of the Brunovistulian margin for the following reasons:

a) apparent lithological similarity with the Vranov-Olešnice Unit, which is intercalated with ca. 600 Ma old Cadomian orthogneisses (Bíteš gneisses — Friedl et al. 2004);

Table 11: K-Ar ages of the gabbroic rocks.

Sample	Rock	Dated mineral	K (%)	$^{40}\text{Ar}(\text{rad}) 10^{-6} \text{ ccSTP/g}^*$	$^{40}\text{Ar}(\text{rad}) \%$	Age $\pm 1\sigma$ (Ma)
M-1b	Olivine norite	Plg	0.224	8.706	77.7	796 \pm 32
M-2	Norite	Plg	0.215	15.960	77.6	1302 \pm 50
M-2		Plg HF treated	0.274	4.037	20.1	344 \pm 25
M-2		Bt	2.687	35.950	91.4	315 \pm 12
M-2		Amp	0.323	8.023	86.9	550 \pm 18
M-2		Amp $> 3.15 \text{ g}\cdot\text{cm}^{-3}$	0.495	9.800	82.5	449 \pm 17
M-2		Amp $> 3.20 \text{ g}\cdot\text{cm}^{-3}$	0.244	6.399	72.4	573 \pm 22
M-3A	Hornblende melagabbro	Amp	0.530	7.864	79.8	346 \pm 13
M-4	Hornblende norite	Amp	0.591	8.773	90.7	346 \pm 13
M-5-1	Hornblende ol. gabbro	Plg	0.171	2.889	60.1	389 \pm 23
M-5-1		Amp	0.346	8.989	89.1	568 \pm 21
M-5-2	Gabbro	Plg	0.115	1.935	71.3	388 \pm 22
M-5-2		Cpx	0.411	4.365	81.2	254 \pm 10
M-5-3	Biotite gabbro	Bt	6.492	87.460	95.5	320 \pm 12
M-5-3		Amp+Cpx	0.332	4.846	71.6	342 \pm 13
M-5-3		Amp $\sim 3.15 \text{ g}\cdot\text{cm}^{-3}$	0.527	6.572	65.3	296 \pm 12
M-5-3		Plg	1.246	13.990	73.4	268 \pm 10
M-6	Two-mica granite	Bt	5.853	80.895	96.7	324 \pm 12

*1 cm³ of gas at standard temperature and pressure

b) the coronitic gabbro from Olešnice (Weiss 1985) in the Svratka window shows the same pattern of corona development and is spatially associated with marbles and garnet amphibolites as coronitic gabbros in the Vratěnin Unit.

The studied gabbroic rocks mostly form small rounded bodies X0 to X00 m in size, strongly differentiated by processes of crystal accumulation, liquid fractionation and assimilation of country rocks. This implies that most bodies represent cumulates of (ultra)mafic composition. Gabbroic cumulates from the Moldanubian Monotonous Unit and the Vratěnin Unit differ in: a) preserved magmatic layering observed only in the Maříž locality, b) their composition: the Maříž samples are Mg-rich, while those from the Vratěnin Unit are Fe-rich (cf. Koller 1998; Matějka & Holub 2003), c) their mineralogy: the Maříž samples mostly contain only orthopyroxene, while those of the Vratěnin Unit are mostly two pyroxene-bearing, d) their textures: coronitic textures are developed only in the Vratěnin Unit.

Ultramafic to mafic cumulate gabbroic complexes with coronitic textures typically occur in medium- to high-pressure amphibolite-granulite facies metamorphic terrains (e.g. de Haas 2002), but olivine-plagioclase coronas were described from low-pressure (up to 1 kbar) domains (Turner & Stuewe 1992). They may be formed either by late magmatic processes during reaction of cumulus phases with hydrous interstitial liquids, or in the solid state due to the activities of fluid-assisted metamorphic processes (Claeson 1998; de Haas et al. 2002; Ikeda et al. 2007; Helmy et al. 2008).

Their tectonomagmatic and metamorphic histories are postdated by the Variscan high-grade metamorphic event (ca. 350–340 Ma) recorded in the Moldanubian Unit and somewhat later also in the underlying Moravian complexes (Fritz & Neubauer 1993; Kotková et al. 2007). Unfortunately, the Sm-Nd isochrone ages fail to give real geological ages, most likely due to variable contamination of gabbros by host rocks. The results of K-Ar dating of different minerals from the coronitic and non-coronitic gabbros show a relict of ca. 570–550 Ma Cadomian ages, but also a strong Variscan imprint, which disturbed the K-Ar isotopic system. Three possible scenarios exist:

1. The gabbroic complexes represent pre-Variscan intrusions involved in the Variscan high-grade metamorphic processes. The presence of coronitic textures only in the Vratěnin Unit reflects different conditions during the Cadomian late magmatic processes — the presence of H₂O-rich late magmatic fluids, rapid exhumation and cooling in the case of coronitic gabbros from the Vratěnin Unit. Mafic to ultramafic complexes with coronitic textures of ca. 570–550 Ma and very similar geochemical and Sm-Nd isotopic characteristics were reported by Cottin et al. (1998) from the Panafrican Belt in Hoggar and the Panafrican Eastern Desert terrane in Egypt (Helmy et al. 2008). Both regions are possible candidates for areas from which the Armorican and Brunovistulian crustal fragments could be derived.

2. The gabbros are pre-Variscan intrusives, possibly Cadomian in age, but coronitic textures originated during the Variscan metamorphic processes connected with underthrusting of the Brunovistulian margin beneath the Moldanubian root. Such processes, in which the intrusive age is much high-

er than that of the coronas, have been reported from the Grenvillian orogen in Canada, Norway, but also from Variscan terrains of the Massif Central, France and Bohemian Massif (Štědrá et al. 2002). This interpretation is supported by the presence of a garnet corona around plagioclase in a solitary sample from Korolupy and replacement of ilmenite with developed amphibole coronas by titanite.

3. Olivine-orthopyroxene coronas could have originated in the magmatic stage in pre-Variscan times because olivine is in textural equilibrium with the magmatic pargasite, which also replaces orthopyroxenes. Fine-grained symplectitic amphibole with spinel grains and scarcely preserved garnet coronas around plagioclase are products of solid-state fluid-assisted metamorphic reactions, which accompanied the dehydration in the host metasediments.

Petrogenesis of the gabbros: mantle and crustal contribution

The geochemical data help to define the petrogenesis of the gabbroic rocks. SiO₂ vs. alkali contents show their subalkaline character (Fig. 7), with the exception of the Mešovice norite and the Maříž (M-5-5) gabbros. The chemical composition of the primary gabbroic rocks should suggest derivation of the primary gabbroic magmas from mantle-sources. The high Mg# numbers and MgO concentrations in most of the samples (Table 9) most likely point to their cumulate origin produced by fractional crystallization, probably in crustal magma chambers. The positive Eu anomalies (Fig. 9A) suggest that plagioclase is a major cumulus phase in these rocks. The evolution of basaltic magmas in the crust is typically accompanied by variable degrees of contamination, namely by the assimilation-fractional crystallization processes outlined by Hildreth & Moorbath (1988). High trace element contents (e.g. light rare earth elements — LREE, large ion lithophile elements — LILE), well developed negative Nb anomalies and distinctly variable Sr-Nd isotopic composition (e.g. ϵ_{Nd} -8.0 to +5.0) of the samples (see Table 10) may suggest either significant contribution by crustal (subduction-related) material in the magma source or (more probably) incorporation of felsic crustal material to the parent magma during its ascent or emplacement.

In order to account for the observed geochemical characteristics we consider two possibilities for their petrogenesis: (1) the magma was derived from enriched upper mantle sources with subduction-related characteristics or (2) primary magma of mantle origin was contaminated during emplacement (underplating) by crustal material and acquired its geochemical characteristics as a result of the assimilation-fractional crystallization process.

In spite of their similar petrography and their present geotectonic position, the Maříž gabbroic rocks are distinctly different from those at Korolupy-Nonndorf and Mešovice. For example, all the Maříž gabbroic rocks have high crust-like La/Nb ratios of 2.1–6.6 (bulk continental crust has La/Nb ratio of 2.5; Rudnick & Gao 2003), coupled with uniform low ϵ_{Nd} values from -0.6 to +0.7 whereas gabbroic rocks from other localities have La/Nb ratios < 1.7 and show negative correlations between La/Nb and ϵ_{Nd} (Fig. 11). Such decoupling between La/Nb (and also $^{87}Sr/^{86}Sr$) and ϵ_{Nd} may be attributed to crustal

contamination by material with high La/Nb (Rudnick & Gao 2003) and/or derivation of the magma from the source with already fractionated La/Nb ratios and decoupled Sr-Nd isotopic composition. This phenomenon is also shown by the differentiated Maříž intrusion. The degree of enrichment of mobile elements (Cs, Ba, Rb, K, Sr etc.) in the Maříž samples is strongly correlated with the radiogenic Sr isotopic compositions. Such geochemical signatures commonly characterize the mantle wedge affected by subduction-related metasomatism (e.g. Keppler 1986; Hawkesworth et al. 1991; Hermann et al. 2006).

Compared to the other samples, the Mešovice norite is distinct in having a positive Nb-anomaly ($Nb_N/Th_N=1.7$) coupled with a very high TiO_2 content (3.4 wt. %; Table 9), an alkaline composition as signified in the TAS (Fig. 7) and a radiogenic ϵ_{Nd} value of +5.0. Positive Nb-anomalies as well as high TiO_2 contents are characteristic of OIB or rift-related basalts free of any subduction component (e.g. Lustrino & Wilson 2007 and references therein). The fact that the Mešovice norite also has a character indicative of a highly incompatible element-depleted mantle source, with highly radiogenic ϵ_{Nd} (+5.0), strongly supports mantle-derived magma emplacement during the continued crustal extension.

The Korolupy-Nonndorf norites have smaller negative Nb-anomalies ($Nb_N/Th_N=0.5-0.8$) than those from Maříž ($Nb_N/Th_N < 0.5$). In spite of having La/Nb ratios and Sr contents similar to those of the Uherčice gabbros, they are significantly poorer in large lithophile elements than the Uherčice gabbros. This suggests that they were only slightly contaminated by crustal material. In contrast, in spite of their similar moderately negative Nb-anomalies and much lower ϵ_{Nd} values (-6 to -8), the Uherčice gabbros show two distinct geochemical patterns: (1) low Rb coupled with a highly non-radiogenic Sr isotopic composition of 0.70275 (Uherčice, M-3B) and (2) large lithophile element enrichment associated with highly radiogenic Sr isotopic composition of 0.71909 (Uherčice, M-3A). This can be interpreted as inherited from assimilation of different crustal materials or more probably, old (e.g.

Nd model ages of 2.5 to 3.0 Ga; Liew & Hofmann 1988), extensively recycled material.

Apparent trends (negative correlations between La/Nb and ϵ_{Nd} and a possible mixing line in the Sr-Nd isotopic diagram) for the Mešovice-Korolupy-Nonndorf-Uherčice rocks suggest that these rocks originated from a single parent magma that was affected by varying degrees of assimilation-fractional crystallization process.

Conclusions

Petrological, geochemical, Sr-Nd isotopic and K-Ar studies of gabbroic cumulates from the Moldanubian Monotonous Unit and the Moravian Vratěnín Unit provide the following constraints on the sources, evolution and age of these rocks:

(1) Both complexes represent pre-Variscan, partly differentiated ultramafic-mafic intrusions of probably Cadomian age (ca. 550–570 Ma), with very similar geochemical and isotopic characteristics. They were emplaced into units of different microcontinent fragments derived from the African part of the Neoproterozoic Avalonian-Cadomian orogen. They were heterogeneously involved in the Variscan collision of the Moldanubian and the Brunovistulian microcontinents. The two-pyroxene thermometry (1000–700 °C) and clinopyroxene-plagioclase barometry (8–5 kbar) performed by Koller (1998) also show a wide scatter of data for these rocks.

(2) Coronitic texture, present in the gabbroic rocks of the Vratěnín Unit, could have originated more probably during both magmatic (orthopyroxene coronas) and/or the solid-state fluid-enhanced metamorphic reactions. Amphibole- and spinel-bearing, scarcely also garnet coronas were produced at contact between symplectitized orthopyroxene and plagioclase. According to the strong amphibolite-facies imprint in some gabbroic samples passing to garnet amphibolites, we assume that amphibole-garnet coronas could have originated during underthrusting of the Brunovistulian margin below the Moldanubian Unit. Later, they were equilibrated in the amphibolite-facies conditions, during exhumation and final imbrication of the Drosendorf stack.

(3) The studied gabbroic rocks crystallized from magma which was derived from moderately depleted mantle sources but enriched by subduction-related fluids before their emplacement. More probably they were differentially contaminated by heterogeneous crustal material in two lithologically distinct crustal units during the emplacement in pre-Variscan times. This would explain the wide range of obtained ϵ_{Nd} values (+5 to -8). Close spatial relation of the gabbroic cumulates to garnet amphibolites and marbles suggest that their emplacement was connected with fragmentation and rifting of a passive margin sequence in the case of the Vratěnín Unit suite. This is supported by the presence of gabbros of alkaline character and positive ϵ_{Nd} values of ca. +5, which suggest a lower contamination by slab fluids or a continental crust assimilation. Their original geochemical characteristics were strongly influenced by the assimilation-fractional crystallization process. The cumulate gabbro complexes are relatively heterogeneous; their example, the Maříž suite, was contaminated by a larger volume of continental crust compared to the Vratěnín Unit.

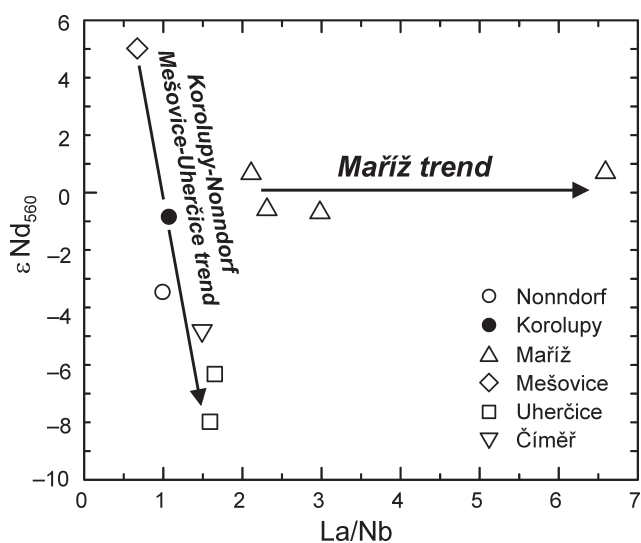


Fig. 11. La/Nb vs. ϵ_{Nd} for the gabbroic rocks.

Acknowledgments: This research was supported by the Grant Agency of the Academy of Sciences CR IAA3013403 within the Research Programme of the Institute of Geology, v.v.i., CEZ: AV0Z30130516 and Research Plan No. MSM0021620855 supported by Ministry of Education, Youth and Sports of the Czech Republic (V. Kachlík). K-Ar dating was supported by OTKA Projects No. T060965 and M41434 to K. Balogh and fission-track studies by IAA300130902 Project to R. Skála. We are indebted to V. Vonásková for whole-rock analyses and L. Strnad for ICP-MS analyses of trace elements, both from Charles University, Prague. The manuscript benefited from comments and criticism by B.G.J. Upton, University of Edinburgh. We are indebted to J. Pavková and V. Sedláček for technical assistance, both of the Institute of Geology AS CR, v.v.i., Prague and reviewers I. Petřík and P. Uher from Bratislava for their comments and improvement of the manuscript.

References

- Balogh K. 1985: K/Ar dating of Neogene volcanic activity in Hungary. Experimental technique, experience and methods of chronological studies. *ATOMKI Report D/1*, Debrecen, 277–278.
- Brey G.P. & Köhler T. 1990: Geothermometry in four-phase lherzolites: II. New thermobarometers, and practical assessment of existing thermobarometers. *J. Petrology* 31, 1352–1378.
- Cháb J., Stráňík Z. & Eliáš M. 2007: Geological Map of Czech Republic 1:500,000. *Czech Geol. Surv.*, Prague.
- Claeson D.T. 1998: Coronas, reaction rims, symplectites and emplacement depth of the Rymmen gabbro, Transscandinavian Igneous Belt, southern Sweden. *Mineral. Mag.* 62, 743–757.
- Cottin J.Y., Lorand J.P., Agrinier P., Bodinier J.L. & Liégeois J.P. 1998: Isotopic (O, Sr, Nd) and trace element geochemistry of the Laouni layered intrusions (Pan-African belt, Hoggar, Algeria): evidence for post-collisional continental tholeiitic magmas variably contaminated by continental crust. *Lithos* 45, 197–222.
- Cox K.G., Bell J.D. & Pankhurst J. 1979: The interpretation of igneous rocks. *Allen and Unwin*, London, 1–450.
- de Haas G.J.L.M., Nijland T.G., Valbracht P.J., Maijer C., Verschure R. & Andersen T. 2002: Magmatic versus metamorphic origin of olivine-plagioclase coronas. *Contr. Mineral. Petrology* 143, 537–550.
- Finger F., Roberts M.P., Hauenschmidt B., Schermaier A. & Steyer H.P. 1997: Variscan granitoids of central Europe: their typology, potential sources and tectonothermal relations. *Miner. Petrology* 61, 67–96.
- Fleet M.E. 2003: Micas. In: Deer W.A., Howie R.A. & Zussman J. (Eds.): Rock-forming minerals. 2nd Ed. *Geol. Soc.*, London, 354–369.
- Franke W. 2000: The mid-European segment of the Variscides: tectonostratigraphic units, terrane boundaries and plate tectonic evolution. In: Franke W., Haak V., Oncken O. & Tanner D. (Eds.): Orogenic processes: Quantification and modeling in the Variscan Belt. *Geol. Soc. London, Spec. Publ.* 179, 337–354.
- Friedl G., Finger F., Paquette J.-L., Quadt A.V., McNaughton N.J. & Fletcher I.R. 2004: Pre-Variscan geological events in the Austrian part of the Bohemian Massif deduced from U-Pb zircon ages. *Int. J. Earth Sci.* 93, 802–823.
- Fritz H. & Neubauer F. 1993: Kinematics of crustal stacking and dispersion in the south-eastern Bohemian Massif. *Geol. Rdsch.* 82, 556–565.
- Gerdes A., Worner G. & Henk A. 2000: Post-collisional granite generation and HT-LP metamorphism by radiogenic heating: the Variscan South Bohemian Batholith. *J. Geol. Soc.* 157, 577–587.
- Harland W.B., Armstrong R.L., Cox A.V., Craig L.E., Smith A.G. & Smith D.G. 1990: A geologic time scale 1989. *Cambridge Univ. Press.*, Cambridge, N.Y., Port Chester, 1–263.
- Hawkesworth C.J., Hergt J.M., McDermott F. & Ellam R.M. 1991: Destructive margin magmatism and the contributions from the mantle wedge and subducted crust. *Austr. J. Earth Sci.* 38, 577–594.
- Hegner E., Walter H.J. & Satir M. 1995: Pb-Sr-Nd isotopic composition and trace element geochemistry of megacrysts and melilitites from the Tertiary Urach volcanic field: source composition of small volume melts under SW Germany. *Contr. Mineral. Petrology* 122, 322–335.
- Helmy H.M., Yoshikawa M., Shibata T., Arai S. & Tamura A. 2008: Corona structure from arc mafic-ultramafic cumulates: The role and chemical characteristics of late-magmatic hydrous liquids. *J. Miner. Petrol. Sci.* 103, 333–344.
- Hermann J., Spandler C., Hack A. & Korsakov A.V. 2006: Aqueous fluids and hydrous melts in high-pressure and ultra-high pressure rocks: Implications for element transfer in subduction zones. *Lithos* 92, 399–417.
- Hildreth W. & Moorbath S. 1988: Crustal contributions to arc magmatism in the Andes of central Chile. *Contr. Mineral. Petrology* 98, 455–489.
- Holland T. & Blundy J. 1994: Non-ideal interactions in calcic amphiboles and their bearing on amphibole-plagioclase thermometry. *Contr. Mineral. Petrology* 116, 433–447.
- Ikeda T., Nishiyama T., Yamada S. & Yanagi T. 2007: Microstructures of olivine-plagioclase corona in meta-ultramafic rocks from Sefuri Mountains, NW Kyushu, Japan. *Lithos* 97, 289–306.
- Jacobsen S.B. & Wasserburg G.J. 1980: Sm-Nd isotopic evolution of chondrites. *Earth Planet. Sci. Lett.* 50, 139–155.
- Jenček V. & Dudek A. 1971: Beziehungen zwischen dem Moravikum und Moldanubikum am Westrand der Thaya-Kuppel. *Věst. Ústř. Úst.* 46, 331–338.
- Keppeler H. 1986: Constraints from partitioning experiments on the composition of subduction-zone fluids. *Nature* 380, 237–240.
- Koller F. 1998: Gabbros and diorites related to the “South Bohemian Pluton”. *Acta Univ. Carol., Geol.* 2, 50.
- Kotkova J., Gerdes A., Parrish R.R. & Novak M. 2007: Clasts of Variscan high-grade rocks within Upper Viséan conglomerates — constraints on exhumation history from petrology and U-Pb chronology. *J. Metamorph. Geology* 25, 781–801.
- Kröner A., Wendt I., Liew T.C., Compston W., Todt W., Fiala J., Vaňková V. & Vaněk J. 1988: U-Pb zircon and Sm-Nd model ages of high-grade Moldanubian metasediments. Bohemian Massif, Czechoslovakia. *Contr. Mineral. Petrology* 99, 257–266.
- Leake B.E. (Ed.) 1997: Nomenclature of amphiboles: Report of the Subcommittee on Amphiboles of the International Mineralogical Association, Commission on New Minerals and Mineral Names. *Amer. Mineralogist* 82, 1019–1037.
- Le Maitre R.W. (Ed.) 2002: Igneous rocks. A classification and glossary of terms. 2nd Ed. *Int. Union Geol. Sci., Cambridge Univ. Press*, Cambridge, 1–236.
- Liew T.C. & Hofmann A.W. 1988: Precambrian crustal components, plutonic associations, plate environment of the Hercynian Fold Belt of central Europe: Indications from a Nd and Sr isotopic study. *Contr. Mineral. Petrology* 98, 129–138.
- Lustrino M. & Wilson M. 2007: The circum-Mediterranean anorogenic Cenozoic igneous province. *Earth Sci. Rev.* 81, 1–65.
- Matějka D. & Holub F. 2003: Olivine-bearing gabbroic rocks of the South Bohemian (Moldanubian) Batholith. *Zpr. Geol. Výzk.* 2002, 171–172 (in Czech).
- Matte P. 2001: The Variscan collage and orogeny (480–290 Ma) and

- the tectonic definition of the Armorica microplate: a review. *Terra Nova* 13, 122-128.
- Merlet C. 1992: Quantitative electron probe microanalysis: new accurate $\Phi(\rho z)$ description. *Mikrochim. Acta* 12, 107-115.
- Morimoto N. 1988: Nomenclature of pyroxenes. *Mineral. Mag.* 52, 535-550.
- Neumann E.-R. 1978: Petrology of the plutonic rocks. In: Dons J.A. & Larsen B.T. (Eds.): The Oslo Paleorift. *Universitetsforlaget*, Trondheim etc., 25-35.
- Nimis P. 1999: Clinopyroxene geobarometry of magmatic rocks. Part 2. Structural geobarometers for basic to acid, tholeiitic and mildly alkaline magmatic systems. *Contr. Mineral. Petrology* 135, 62-74.
- Odin G.S. (Ed.) 1982: Interlaboratory standards for dating purposes. In: Odin G.S. (Ed.): Numerical dating in stratigraphy. *Wiley & Sons*, Chichester etc., 123-149.
- Pitcher W.S. 1978: The anatomy of a batholith. *J. Geol. Soc. London* 135, 157-182.
- Racek M., Stipska P., Pitra P., Schulmann K. & Lexa O. 2006: Metamorphic record of burial and exhumation of orogenic lower and middle crust: a new tectonothermal model for the Drosendorf window (Bohemian Massif, Austria). *Miner. Petrology* 86, 221-251.
- Rudnick R.L. & Gao S. 2003: Composition of continental crust. In: Rudnick R.L. (Ed.): Treatise in geochemistry. *The Crust. Elsevier Pergamon*, Amsterdam, 3, 1-64.
- Schulmann K., Kroner A., Hegner E., Wendt I., Konopasek J., Lexa O. & Stipska P. 2005: Chronological constraints on the pre-orogenic history, burial and exhumation of deep-seated rocks along the eastern margin of the Variscan Orogen, Bohemian Massif, Czech Republic. *Amer. J. Sci.* 305, 407-448.
- Smith J.V. 1974: Feldspar minerals. 1. Crystal structure and physical properties. *Springer*, Berlin etc., 1-627.
- Steiger R.H. & Jäger E. 1977: Subcommission on geochronology: convention on the use of decay constants in geo- and cosmochronology. *Earth Planet. Sci. Lett.* 12, 359-362.
- Strnad L., Mihaljevič M. & Šebek O. 2005: Laser ablation and solution ICP-MS determination of rare earth elements in USGS BIR-1G, BHVO-2G and BCR-2G glass reference material. *Geostand. Geoanal. Res.* 29, 303-314.
- Sun S.S. & Mc Donough W.F. 1989: Chemical and isotopic systematics of oceanic basalts. Implication for mantle composition and processes. In: Saunders A.D. & Norry M.J. (Eds.): Magmatism in the Ocean basins. *Geol. Soc., Spec. Publ.* 42, 313-345.
- Štědrá V., Kachlík V. & Kryza R. 2002: Coronitic metagabbros of the Mariánské Lázně Complex and Teplá Crystalline Unit: inferences for the tectonometamorphic evolution of the western margin of the Teplá Barrandian Unit, Bohemian Massif. In: Winchester J., Pharaoh T. & Verniers J. (Eds.): Palaeozoic amalgamation of Central Europe. *Geol. Soc. London, Spec. Publ.* 201, 217-236.
- Tollmann A. 1982: Großräumiger variszischer Deckenbau im Moldanubikum und neue Gedanken zum Variszikum Europas. *Geotekt. Forsch.* 64, 1-91.
- Turner S.P. & Stuewe K. 1992: Low-pressure corona textures between olivine and plagioclase in unmetamorphosed gabbros from Black Hill, south Australia. *Mineral. Mag.* 56, 503-509.
- Vorma A. 1976: On the petrochemistry of rapakivi granite, with special reference to the Laitila massif, southwestern Finland. *Bull. Geol. Surv. Finland* 285, 125-140.
- Weiss J. 1986: Petrography of basic rocks west of Olešnice at Moravia. *Sbor. Úst. Úst. Geol. Odd. Geol.* 23, 29-58 (in Czech).